Theses and Dissertations | 1. Thesis and Dissertation Collection, all items

1973

Radio direction finding fix solution in spherical trigonometry with confidence region and location error analysis.

Potts, Ronald Lee.

Monterey, California. Naval Postgraduate School

http://hdl.handle.net/10945/16770

RADIO DIRECTION FINDING FIX SOLUTION
IN SPHERICAL TRIGONOMETRY WITH CONFIDENCE
REGION AND LOCATION ERROR ANALYSIS

Ronald Lee Potts

NAVAL POSTGRADUATE SCHOOL
Monterey, California

THESIS

RADIO DIRECTION FINDING FIX SOLUTION
IN SPHERICAL TRIGONOMETRY WITH CONFIDENCE
REGION AND LOCATION ERROR ANALYSIS

by

Ronald Lee Potts

Thesis Advisor: Robert R. Read

March 1973

Radio Direction Finding Fix Solution in Spherical
Trigonometry with Confidence Region and Location Error Analysis

by

Ronald Lee Potts
Lieutenant, United States Navy
B.A., Miami University, 1965

Submitted in partial fulfillment of the
requirements for the degree of

MASTER OF SCIENCE IN OPERATIONS RESEARCH

from the

NAVAL POSTGRADUATE SCHOOL
March 1973

ABSTRACT

Although parts of this paper may be applicable to various
other location finding systems, radio direction finding was
selected for development because of the extensive literature
available on the subject. Using a modification of the navi-
gation coordinate system, equations in spherical trigonometry
are developed by analogy with graphical solution procedures.
Ellipticity of the earth is corrected for by use of geocen-
tric latitude in all calculations. The least squares solu-
tion is found by a combination of second-order gradient
searches and Golden Section Searches on the corrected sphere.
A Chi-Square contour confidence region is presented with
defense against the empty region arguments and with verifi-
cation of its reliability of target containment. Sensitivity
of location error to network layout, number of measurements
available and intercept geometry factors is examined by
computer simulation, demonstrating the predictive value of
these statistics. It is shown that the correlation between
location error and the size of a reliable confidence region
is too minimal to have predictive value.

2

TABLE OF CONTENTS

LIST OF FIGURES

6

I. INTRODUCTION

Various procedures have been described for estimating an
emitter location from a set of measured signal azimuths
reported to a control station by dispersed direction finding
(DF) sites. Such procedures range upward in complexity from
visual estimates off a plot of great circle arcs on a
gnomonic projection of the operating area of potential
targets. Other procedures exist for describing confidence
criteria about the location estimate. The present paper was
motivated by an interest in confidence regions and in loca-
tion error analysis. Such studies require either that the
procedure used be free of approximating assumptions, or that
the variability of the approximations be included in the
confidence criterion. The former course was preferred for
simplicity and consistency of estimates. This paper presents
an emitter location estimate procedure based only upon known
DF site coordinates and signal azimuths. The procedure
described in sections II and III converges quickly to a
least squares solution and does not require an initialization
point estimate of the location from external sources (Pope,
1971). The procedure does not require a rejection of out-
liers (McCalla, 1970) in order to converge to the least
squares solution. The approach is free from assumptions in
the categories that the earth is flat in the solution region,
that the earth is a perfect sphere, that great circle arcs

are well enough approximated by straight lines of position, and that azimuth errors are well enough approximated by parallel displacements of such lines of position (Daniels, 1951).

Section IV describes a Chi-Square contour confidence region procedure. Factors from intercept geometry are discussed in section V. Section VI is a description of procedures used to simulate the problem for the purpose of the location error analyses described in sections VII and VIII. An alternative to confidence regions for predicting location accuracy is discussed in the concluding section.

II. MATHEMATICAL DESCRIPTION OF SPATIAL RELATIONSHIPS

Locations and spatial relationships of interest in direction finding and target fixing can be expressed completely in spherical trigonometry. The advantage of such expression is that each mathematical step has its simple graphical counterpart. This paper contains notational and descriptive departures from other direction finding models based on spherical trigonometry. Such notational changes follow those used in geodesy for describing locations and spatial relationships and those used in textbooks on spherical trigonometry for developing equations to express such relationships. Fquations are restricted to sine and cosine functions only in order to simplify calculating first and second order derivatives of somewhat lengthy equations.

A. GLOBAL COORDINATE SYSTEM

The coordinate system is a slight modification of the system used in mapping. Longitude, denoted λ, is measured from zero at the prime meridian eastward through 360 degrees. Latitude, denoted ϕ, is measured from zero at the equator northward through ninety degrees and southward through minus ninety degrees. Azimuth, denoted θ, is measured from zero at true north clockwise through 360 degrees. Such a coordinate system is sufficient to represent any point on the globe as well as the great circles which represent ideal wave propagation paths. Mathematical descriptions of spatial

relationships must account for the longitude discontinuity
at the prime meridian and for the azimuth discontinuity at
true north. A great circle arc with azimuth angle indicated
is sketched on the coordinate system in Figure 1.
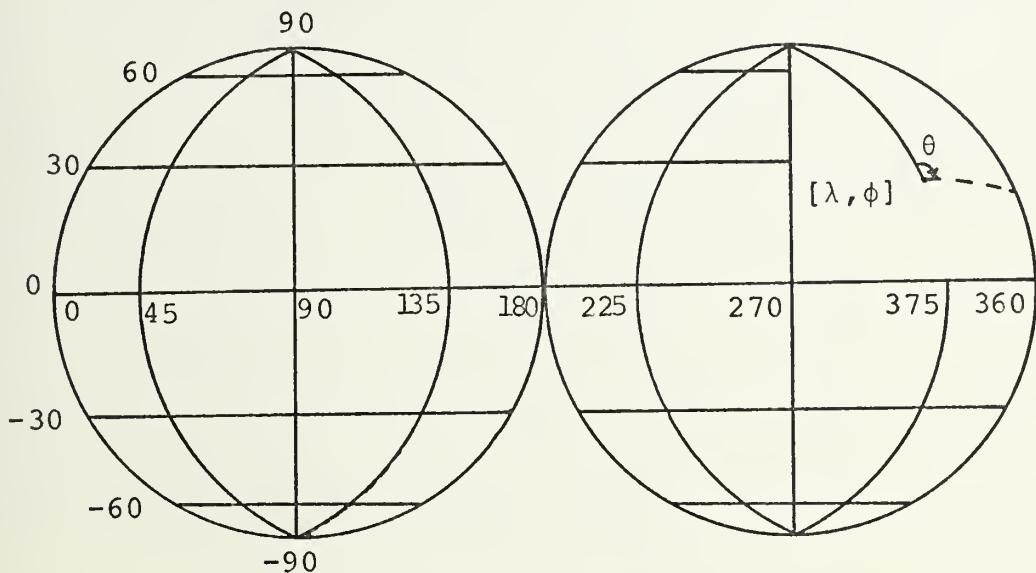
Global Coordinate System

FIGURE 1

B. GEOCENTRIC LATITUDE

Geographical latitude, used in navigation and mapping,
is based upon astronomical observations and mathematical
deductions that do not correct for the ellipticity of the
earth. Consequently, geographical latitude is slightly
greater in magnitude than the arc on a meridian from the
equator to a location with vertex angle at the center of the
earth. Rules of spherical trigonometry can be more accurately
applied to describe spatial relationships following the con-
version from geographical latitude to geocentric, or earth-

10

centered, latitude. Assuming that waves propagate along

great circle arcs, then no information is lost since such

paths are geometrically independent of radii to the earth

center from both the signal emitter and from the DF site.

The maximum discrepancy between the two types of latitude

occurs at ±45 degrees latitude and is about equal to 11.5

minutes of arc. Although the conversion equation appears

in books on geodesy, a derivation could not be found, so the

equation was derived for reference purposes.

In Figure 2, a and b represent the semi-major and semi-

minor axes of the ellipsoid. The point $P(x_1, y_1)$ represents

any point on the ellipsoid. The line OP connects P to the

origin at O, the earth center. SP is perpendicular to the

Equation of ellipse:

$$\frac{x^2}{a^2} + \frac{y^2}{b^2} = 1$$
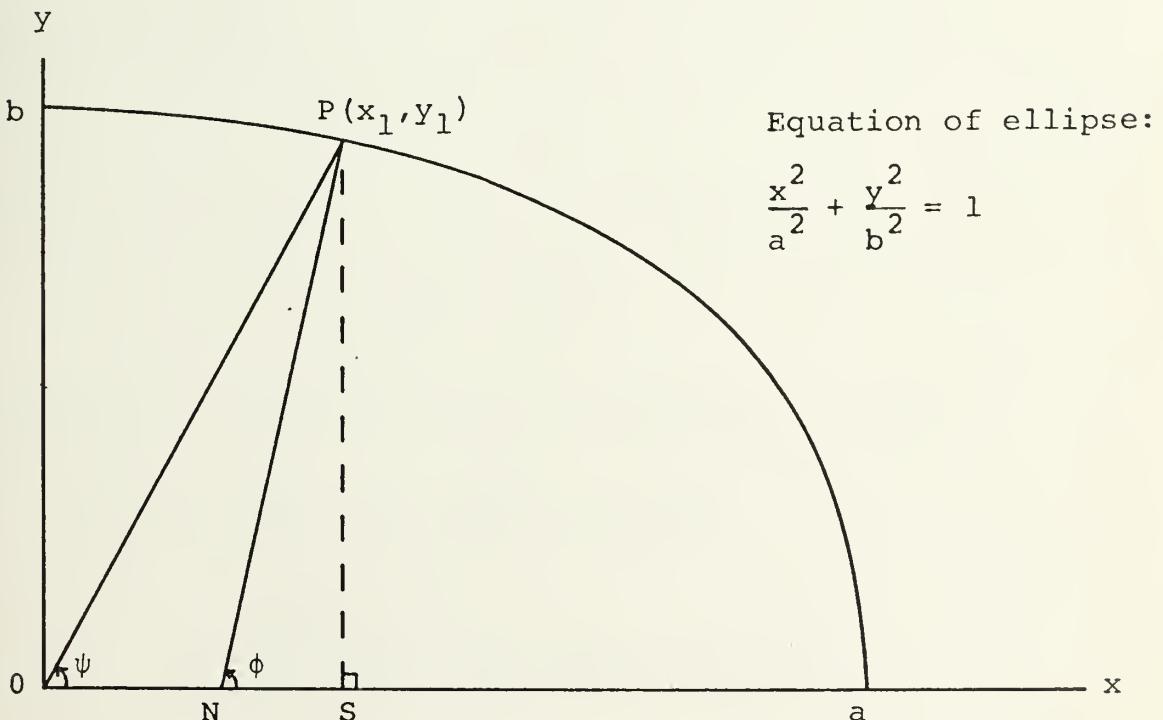
Relationship Between Geographical and Geocentric Latitude

FIGURE 2

11

equatorial plane, the x-axis. NP is the normal line to the ellipsoid at P, and the angle PNS is equivalent to geographical latitude. Angle PON is equivalent to geocentric latitude, denoted ψ. Ellipticity of the quadrant is exaggerated in order to distinguish the two angles.

From Figure 2, it can be seen that

$$SP = OS \tan \psi, \text{ and that } SP = NS \tan\phi,$$

so that

$$\tan\psi = \frac{NS}{OS} \tan\phi \qquad (2-1)$$

From the equation of the ellipse,

$$y_1 = \frac{b}{a} (a^2 - x_1^2)^{\frac{1}{2}} \qquad (2-2)$$

The equation of the normal line NP is given by

$$y - y_1 = - \frac{1}{f'(x_1)} (x - x_1) \qquad (2-3)$$

Differentiating equation (2-2) to solve $f'(x_1)$,

$$f'(x_1) = - \frac{b}{a} x_1 (a^2 - x_1^2)^{-\frac{1}{2}}$$

Substituting in equation (2-3) and rearranging terms,

$$y - y_1 = \frac{a}{bx_1} (a^2 - x_1^2)^{\frac{1}{2}} (x - x_1)$$

$$= \frac{a^2 y_1}{b^2 x_1} (x - x_1), \text{ from equation (2-2).}$$

Then at $y = 0$, y_1 can be cancelled from both sides, and

12

$$\frac{x - x_1}{x_1} = - \frac{b^2}{a^2}$$

From Figure 2, $x_1 = OS$, and at $y = 0$, $x = ON$, so that $x_1 - x = NS$.

$$\frac{NS}{OS} = \frac{b^2}{a^2}$$

Substituting this last result in equation (2-1),

$$\tan\psi = \frac{b^2}{a^2} \tan\phi \qquad\qquad (2\text{-}4)$$

The conversion is usually stated as a function of earth eccentricity,

$$e = \frac{1}{a} (a^2 - b^2)^{\frac{1}{2}}$$

Then

$$e^2 = \frac{a^2 - b^2}{a^2}$$

$$= 1 - \frac{b^2}{a^2}.$$

Therefore,

$$\frac{b^2}{a^2} = 1 - e^2, \text{ and it follows that}$$

$$\tan\psi = (1 - e^2) \tan\phi \qquad\qquad (2\text{-}5)$$

Using $e = 0.081813$ from the International Ellipsoid of Reference (reference 3),

$$\tan\psi = 0.99327733 \tan\phi \qquad\qquad (2\text{-}6)$$

13

C. THE POLAR TRIANGLE

The mathematical description of spatial relationships is based upon a polar triangle constructed from the great circle arcs (measured by the angle subtended by the arc at the earth's center) connecting a DF site, any other point and the north pole. Such a triangle is sketched in Figure 3. The DF site is located at vertex B. Vertex C is at any other point. Vertex A is at the north pole. The arc c is the complement of the geocentric latitude of the DF site. Similarly, the arc b is the complement of the geocentric latitude of the other point. Angle A is equal to the difference in longitude between the DF site and the point. The dotted arc included on Figure 3 corresponds to a signal azimuth with angle indicated by θ.
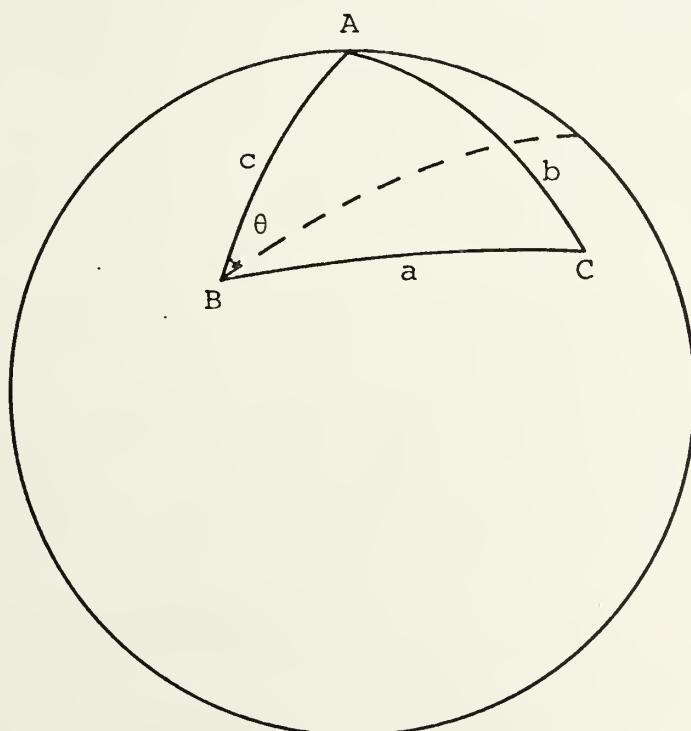
Polar Triangle with Signal Azimuth

FIGURE 3

14

Angle A corresponds to the smaller of two possible polar triangles connecting any two points and the north pole. Visually, there is no problem in deciding which polar triangle to choose. However, when this triangle contains the prime meridian, the discontinuity at longitude 360 = longitude 0 results in assigning the value of the vertex of the larger polar triangle when the longitude difference is taken. The mathematical model can be forced to correspond to the spatial relationships by adding the proviso that if the difference in degrees of longitude is greater than 180 degrees, then let A equal 360 degrees minus the difference. This restricts the size of angle A to one hemisphere. The absolute value of the difference can be taken in case the DF site is east of (greater longitude than) the point. These relationships are summarized below with subscript s designating the DF site and subscript t designating any test point.

$$c = 90 - \psi_s \tag{2-7}$$

$$b = 90 - \psi_t \tag{2-8}$$

$$A = \begin{cases} |\lambda_t - \lambda_s|, & \text{if } |\lambda_t - \lambda_s| \leq 180 \\ \\ 360 - |\lambda_t - \lambda_s|, & \text{if } |\lambda_t - \lambda_s| > 180 \end{cases} \tag{2-9}$$

1. Point Azimuth Solution

The value of arc a connecting the DF site and test point is given by the law of cosines for sides,

$$\cos a = \cos b \cos c + \sin b \sin c \cos A \tag{2-10}$$

15

There is no quadrant ambiguity since the cosine takes nega-
tive values in the second quadrant and arc a is always less
than or equal to 180 degrees because of the restriction on
angle A to one hemisphere. Since the cosine of angle A is
of interest in determining arc a, both the absolute value
sign and the condition can be removed by applying a reduction
formula. From equation (2-9),

$$\cos A = \begin{cases} \cos |\lambda_t - \lambda_s| \\ \\ \cos (360 - |\lambda_t - \lambda_s|), & \text{if } |\lambda_t - \lambda_s| > 180 \end{cases}$$

But, through reduction,

$$\cos (360 - |\lambda_t - \lambda_s|) = \cos |\lambda_t - \lambda_s|$$

The absolute value sign can be dropped since $\cos (\lambda_t - \lambda_s) =$
$\cos (\lambda_s - \lambda_t)$. From this result and equation (2-10)

$$\cos a = \cos b \cos c + \sin b \sin c \cos (\lambda_t - \lambda_s) \qquad (2-11)$$

The vertex angle B at the DF site can be found by applying
one of the laws of cosines for sides,

$$\cos B = \frac{\cos b - \cos c \cos a}{\sin c \sin a} \qquad (2-12)$$

Equation (2-12) is valid for test points either east or west
of the DF site at vertex B.

In order to make comparisons with a signal azimuth,
angle B must be converted to an azimuth from true north,
denoted β. Visually, the conversion is based on whether the
test point is eastward or westward of the DF site with res-
pect to the proper polar triangle. Mathematically, the

16

conversion is based on the magnitude of the longitudes of the DF site and the test point, but must also account for the discontinuity at the prime meridian. There are four general cases with two distinct outcomes as illustrated in Figure 4.

2. Point Azimuth and Signal Azimuth Difference

From a given DF site, the difference between the azimuth of any test point and a signal azimuth is the smaller of the two possible outcomes, depending upon whether the difference is measured clockwise or counter-clockwise. The azimuth difference is denoted ω, and the azimuth discontinuity at true north requires that the computation be conditional. With a clockwise rotation for the azimuths, the smaller angle of azimuth difference will be positive if β is leading and negative if β trails θ. The possible outcomes and their conditions are as follows.

a. If $|\beta - \theta| < 180$, then $\omega = \beta - \theta$

b. If $|\beta - \theta| > 180$ and $\beta > \theta$, then $\omega = \beta - \theta - 360$

c. If $|\beta - \theta| > 180$ and $\beta < \theta$, then $\omega = \beta - \theta + 360$

$$(2-14)$$

The sets of conditions on computing β (B) in equation (2-13) and in computing $\omega(\beta,\theta)$ in equation (2-14) yield six possible outcomes for computing azimuth difference as a function of the vertex angle B and signal azimuth θ.

17
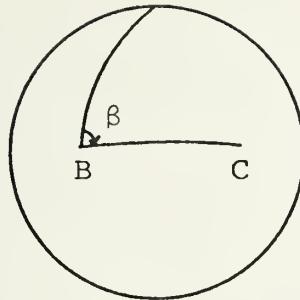
a. $\lambda_s < \lambda_t$ and $\lambda_t - \lambda_s < 180$, then $\beta = B$
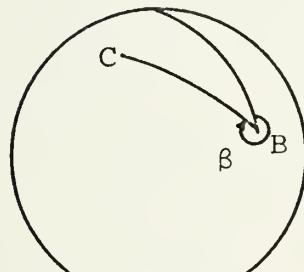
b. $\lambda_s > \lambda_t$ and $\lambda_s - \lambda_t < 180$, then $\beta = 360 - B$
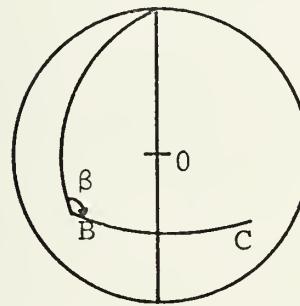
c. $\lambda_s > \lambda_t$ and $\lambda_s - \lambda_t > 180$, then $\beta = B$
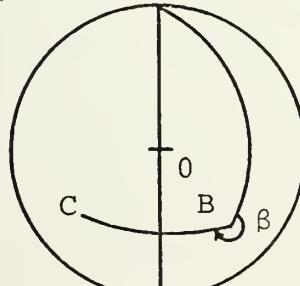
d. $\lambda_s < \lambda_t$ and $\lambda_t - \lambda_s > 180$, then $\beta = 360 - B$

Azimuth and Vertex Angle

FIGURE 4

$$\omega = \begin{cases} B - \theta \\ B - 360 - \theta \\ B + 360 - \theta \\ -B + 360 - \theta \\ -B - \theta \\ -B + 720 - \theta \end{cases}$$

Two utility variables may be introduced in order to express azimuth difference in a constant form with values dependent upon the existing conditions.

$$\omega = pB + q - \theta \tag{2-15}$$

The pair of utility variables can take on any one of the following sets of values

$$(p,q) = \begin{cases} (1,0) \\ (1,-360) \\ (1,360) \\ (-1,360) \\ (-1,0) \\ (-1,720) \end{cases}$$

Concluding development, angle B can be expressed as a differentiable function of sines and cosines of known values of longitude and geocentric latitude. From equations (2-11) and (2-12) and the application of an angle-difference relation,

19

$$B = \cos^{-1}\left[\left(\cos\,b - \cos\,c\,[\cos\,b\,\cos\,c + \sin\,b\,\sin\,c\right.\right.$$

$$(\cos\,\lambda_t\,\cos\,\lambda_s + \sin\,\lambda_t\,\sin\,\lambda_s)]\Big) \Big/ \Big[\sin\,c$$

$$\sin\left(\cos^{-1}[\cos\,b\,\cos\,c + \sin\,b\,\sin\,c\,(\cos\,\lambda_t\,\cos\lambda_s\right.$$

$$\left.\left.+ \sin\,\lambda_t\,\sin\,\lambda_s)]\right)\Big]\right]$$

Substituting the values for arcs b and c from equations (2-7) and (2-8) and using the reduction formulas cos (90 - x) = sin x and sin (90 - x) = cos x,

$$B = \cos^{-1}\left[\left(\sin\,\psi_t - \sin\,\psi_s\,[\sin\,\psi_t\,\sin\,\psi_s + \cos\,\psi_t\right.\right.$$

$$\cos\,\psi_s\,(\cos\,\lambda_t\,\cos\,\lambda_s + \sin\,\lambda_t\,\sin\,\lambda_s)]\Big) \Big/ \Big[\cos\,\psi_s$$

$$\sin\left(\cos^{-1}[\sin\,\psi_t\,\sin\,\psi_s + \cos\,\psi_t\,\cos\,\psi_s\,(\cos\,\lambda_t\right.$$

$$\left.\left.\cos\,\lambda_s + \sin\,\lambda_t\,\sin\,\lambda_s)]\right)\Big]\right]$$

By multiplying the term $\sin\,\psi_s$ through the interior brackets of the numerator, writing the first two resulting terms as $\sin\,\psi_t\,(1 - \sin^2\psi_s)$, which is equal to $\sin\,\psi_t\,\cos^2\psi_s$, $\cos\,\psi_s$ can be cancelled from both numerator and denominator.

$$B = \cos^{-1}\left(\left[\sin\,\psi_t\,\cos\,\psi_s - \sin\,\psi_s\,\cos\,\psi_t\,(\cos\,\lambda_t\right.\right.$$

$$\cos\,\lambda_s + \sin\,\lambda_t\,\sin\,\lambda_s)\Big] \Big/ \Big[\sin\left(\cos^{-1}\Big[\sin\,\psi_t\right.$$

$$\sin\,\psi_s + \cos\,\psi_t\,\cos\,\psi_s\,(\cos\,\lambda_t\,\cos\,\lambda_s$$

$$\left.\left.+ \sin\,\lambda_t\,\sin\,\lambda_s)\Big]\right)\Big]\right) \qquad\qquad (2\text{-}16)$$

III.   THE FIX SOLUTION

In Figure 5, each of four DF sites have measured azimuths of a signal from the same emitter at an unknown location. The signal azimuths are plotted for illustration as dotted arcs.   A test point, $\bar{P}(\lambda_t, \psi_t)$, is established, and azimuths from each DF site to $\bar{P}$ are drawn in solid arcs.   A better fit can be found by moving $\bar{P}$ somewhere within the region bounded by the dotted arcs.

Given a number n of DF sites, each reporting the azimuth of a received signal with respect to its own location to a net control, the fix problem can be viewed as finding the
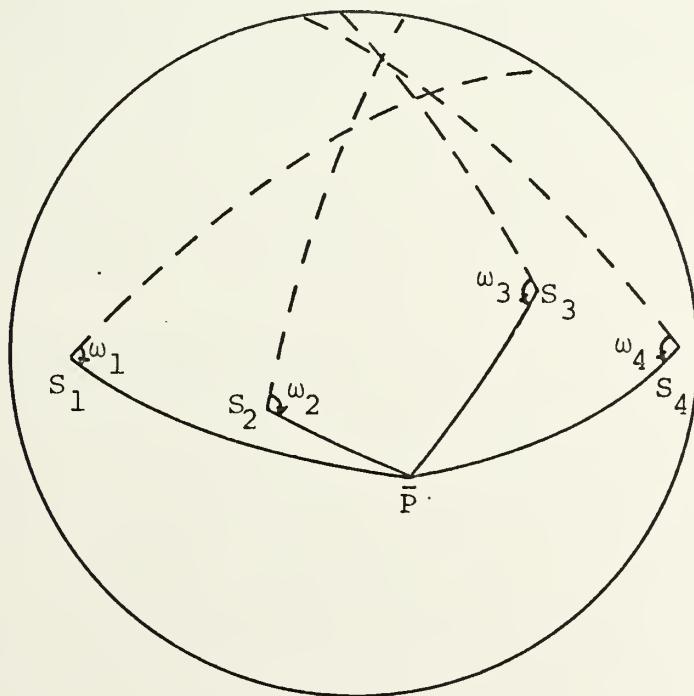
Azimuth Differences

FIGURE 5

point on the globe which minimizes the sum of some function
of the azimuth differences ω_i, for $i = 1, 2, \ldots, n$.

A. OBJECTIVE FUNCTION

Since the azimuth differences are signed, minimizing
their sum may produce a solution that lies outside the region
bounded by arcs corresponding to signal azimuths when large
positive and large negative azimuth differences cancel each
other out. Minimizing the sum of the absolute values of
azimuth differences avoids this problem of positive and
negative differences; however, since the partial derivatives
of absolute value are not computationally tractable, solution
techniques are limited. Minimizing the sum of the squared
azimuth differences provides an objective function that is
differentiable and reflects absolute magnitude. Therefore,
the solution of the fix problem is taken to be that pair of
coordinates (λ_t, ψ_t) which will

$$\text{Minimize} \quad \sum_{i=1}^{n} \omega_i^2 \, (\lambda_t, \psi_t) \qquad\qquad (3-1)$$

B. SECOND-ORDER GRADIENT SEARCH

Dropping the t subscript to simplify exposition, the
objective function, equation (3-1), can be represented as
$f(\lambda, \psi)$. Given an initial test point (λ, ψ), a truncated
Taylor's series for a function of two variables can be used
to approximate the functional values of other test points
$(\lambda + \Delta\lambda, \, \psi + \Delta\psi)$.

22

$$f(\lambda + \Delta\lambda, \ \psi + \Delta\psi) \doteq f(\lambda,\psi) + \Delta\psi \ \frac{\partial f(\lambda,\psi)}{\partial\psi} + \Delta\lambda \ \frac{\partial f(\lambda,\psi)}{\partial\lambda}$$

$$+ \ \frac{1}{2}(\Delta\lambda)^2 \ \frac{\partial^2 f(\lambda,\psi)}{\partial\lambda^2} + \Delta\lambda\Delta\psi \ \frac{\partial^2 f(\lambda,\psi)}{\partial\lambda\partial\psi} + \frac{1}{2}(\Delta\psi)^2 \ \frac{\partial^2 f(\lambda,\psi)}{\partial\psi^2}$$

Expressing the approximation in matrix form and letting superscript t indicate the transpose,

$$f\begin{pmatrix} \lambda + \Delta\lambda \\ \psi + \Delta\psi \end{pmatrix} \doteq f(\lambda,\psi)^t + (\Delta\lambda, \Delta\psi) \begin{pmatrix} \dfrac{\partial f(\lambda,\psi)}{\partial\lambda} \\ \dfrac{\partial f(\lambda,\psi)}{\partial\psi} \end{pmatrix}$$

$$+ \ \frac{1}{2}(\Delta\lambda,\Delta\psi) \begin{pmatrix} \dfrac{\partial^2 f(\lambda,\psi)}{\partial\lambda^2} & \dfrac{\partial^2 f(\lambda,\psi)}{\partial\lambda\partial\psi} \\[2mm] \dfrac{^2 f(\lambda,\psi)}{\partial\lambda\partial\psi} & \dfrac{^2 f(\lambda,\psi)}{\partial\psi^2} \end{pmatrix} \begin{pmatrix} \Delta\lambda \\ \Delta\psi \end{pmatrix}$$

Letting $\bar{P}_j$ denote an initial test point $(\lambda,\psi)^t$, letting $\bar{R}$ denote the vector $(\Delta\lambda,\Delta\psi)^t$, letting ∇ denote the gradient of $f(\bar{P}_j)$ and letting ∇^2 denote the Hessian matrix of f at $\bar{P}_j$, the approximation can be expressed as

$$f(\bar{P}_j + \bar{R}) \doteq f(\bar{P}_j) + \bar{R}^t \nabla f(\bar{P}_j) + \frac{1}{2} \bar{R}^t \nabla^2 f(\bar{P}_j) \ \bar{R}$$

Then,

$$f(\bar{P}_j + \bar{R}) - f(\bar{P}_j) \doteq \bar{R}^t \nabla f(\bar{P}_j) + \frac{1}{2} \bar{R}^t \nabla^2 f(\bar{P}_j) \ \bar{R} \qquad (3\text{-}2)$$

Starting from an initial test point at $\bar{P}_j$, the search procedure can be understood as a technique to find a vector $\bar{R}$ such that $f(\bar{P}_j + \bar{R})$ is the minimum of the objective function. Such a vector $\bar{R}$ also minimizes the left hand side of equation (3-2). Since the quadratic form on the right hand side is an

approximation of the value of the left hand side, it must

be near a minimum value when the left hand side is minimized.

The approximation works both ways, so that a vector $\bar{R}$ which

minimizes the right hand side must approximately minimize

the left hand side. The right hand side is in a form that

yields to analysis of its extreme values with respect to $\bar{R}$

at a fixed $\bar{P}_j$. One of the conditions necessary for the

quadratic form to be at a minimum is that its gradient be

equal to zero. Therefore, it is necessary to find a vector

$\bar{R}$ which fulfills this condition. Taking the gradient of

equation (3-2) with respect to $\bar{R}$,

$$\nabla_{\bar{R}}\left[\bar{R}^t \nabla f(\bar{P}_j) + \frac{1}{2}\bar{R}^t \nabla^2 f(\bar{P}_j)\ \bar{R}\right]$$

$$= \nabla_{\bar{R}}\left[\bar{R}^t \nabla f(\bar{P}_j)\right] + \nabla_{\bar{R}}\left[\frac{1}{2}\bar{R}^t \nabla^2 f(\bar{P}_j)\ \bar{R}\right]$$

$$= \nabla f(\bar{P}_j) + \frac{1}{2}\nabla^2 f(\bar{P}_j)\ \bar{R} + \frac{1}{2}\bar{R}^t \nabla^2 f(\bar{P}_j)$$

$$= \nabla f(\bar{P}_j) + \nabla^2 f(\bar{P}_j)\ \bar{R}$$

Setting the gradient of the quadratic form at $\bar{R}$ equal to zero,

$$\nabla f(\bar{P}_j) + \nabla^2 f(\bar{P}_j)\ \bar{R} = 0$$

Then,

$$\nabla^2 f(\bar{P}_j)\ \bar{R} = -\nabla f(\bar{P}_j)$$

And, providing that $\nabla^2 f(\bar{P}_j)$ is invertible,

$$\bar{R} = -\left[\nabla^2 f(\bar{P}_j)\right]^{-1} \nabla f(\bar{P}_j) \qquad (3-3)$$

24

$\bar{R}$ specifies both a direction and magnitude in which to move toward an extreme value of the objective function. This consequence of the Taylor approximation can be improved by applying a scalar coefficient, denoted δ, to $\bar{R}$ in order to adjust the magnitude and, if $\bar{R}$ points to a maximum value, the direction. The next test point is then given by

$$\bar{P}_{j+1} = \bar{P}_j + \delta\bar{R} \tag{3-4}$$

Combining equations (3-3) and (3-4),

$$\bar{P}_{j+1} = \bar{P}_j - \delta\left[\nabla^2 f(\bar{P}_j)\right]^{-1}\nabla f(\bar{P}_j) \tag{3-5}$$

The search procedure can be terminated when further improvements are of little consequence, most readily determined by comparing the distance between locations on successive iterations.

In order to solve equation (3-5), it is necessary to compute the inverse Hessian of the objective function.

$$\left[\nabla^2 f(\bar{P})\right]^{-1} = \frac{1}{\det\left[\nabla^2 f(\bar{P})\right]}\begin{pmatrix} \dfrac{\partial^2 f(\bar{P})}{\partial\psi^2} & -\dfrac{\partial^2 f(\bar{P})}{\partial\lambda\partial\psi} \\[2ex] -\dfrac{\partial^2 f(\bar{P})}{\partial\lambda\partial\psi} & \dfrac{\partial^2 f(\bar{P})}{\partial\lambda^2} \end{pmatrix}$$

where the determinant of the Hessian

$$\det\left[\nabla^2 f(\bar{P})\right] = \frac{\partial^2 f(\bar{P})}{\partial\lambda^2}\ \frac{\partial^2 f(\bar{P})}{\partial\psi^2} - \left[\frac{\partial^2 f(\bar{P})}{\partial\lambda\partial\psi}\right]^2$$

Substituting the inverse Hessian in equation (3-5) and expanding the equation by matrix multiplication of the inverse Hessian times the gradient yields a new test point with δ the only unknown.

25

$$\bar{P}_{j+1} = \bar{P}_j - \delta \left(\begin{array}{c} \dfrac{\dfrac{\partial^2 f(\bar{P}_j)}{\partial \psi^2} \dfrac{\partial f(\bar{P}_j)}{\partial \lambda} - \dfrac{\partial^2 f(\bar{P}_j)}{\partial \lambda \partial \psi} \dfrac{\partial f(\bar{P}_j)}{\partial \psi}}{\dfrac{\partial^2 f(\bar{P}_j)}{\partial \lambda^2} \dfrac{\partial^2 f(\bar{P}_j)}{\partial \psi^2} - \left(\dfrac{\partial^2 f(\bar{P}_j)}{\partial \lambda \partial \psi} \right)^2} \\[3em] \dfrac{\dfrac{\partial^2 f(\bar{P}_j)}{\partial \lambda^2} \dfrac{\partial f(\bar{P}_j)}{\partial \psi} - \dfrac{\partial^2 f(\bar{P}_j)}{\partial \lambda \partial \psi} \dfrac{\partial f(\bar{P}_j)}{\partial \lambda}}{\dfrac{\partial^2 f(\bar{P}_j)}{\partial \lambda^2} \dfrac{\partial^2 f(\bar{P}_j)}{\partial \psi^2} - \left(\dfrac{\partial^2 f(\bar{P}_j)}{\partial \lambda \partial \psi} \right)^2} \end{array} \right)$$

(3-6)

The solution of equation (3-6) in turn requires the calculation of all first and second partial derivatives of the objective function.

$$\frac{\partial f(\bar{P})}{\partial \lambda} = \frac{\partial \left(\sum\limits_{i=1}^{n} \omega_i^2 \right)}{\partial \lambda}$$

$$= \sum_{i=1}^{n} 2p_i (p_i B_i + q_i - \theta_i) \frac{\partial B_i}{\partial \lambda}$$ (3-7)

Similarly,

$$\frac{\partial f(\bar{P})}{\partial \psi} = \sum_{i=1}^{n} 2p_i (p_i B_i + q_i - \theta_i) \frac{\partial B_i}{\partial \psi}$$ (3-8)

$$\frac{\partial^2 f(\bar{P})}{\partial \lambda^2} = \sum_{i=1}^{n} \left[2p_i^2 \left(\frac{\partial B_i}{\partial \lambda} \right)^2 + 2p_i (p_i B_i + q_i - \theta_i) \frac{\partial^2 B_i}{\partial \lambda^2} \right]$$ (3-9)

$$\frac{\partial^2 f(\bar{P})}{\partial \psi^2} = \sum_{i=1}^{n} \left[2p_i^2 \left(\frac{\partial B_i}{\partial \psi} \right)^2 + 2p_i (p_i B_i + q_i - \theta_i) \frac{\partial^2 B_i}{\partial \psi^2} \right]$$ (3-10)

$$\frac{\partial^2 f(\bar{P})}{\partial \lambda \partial \psi} = \sum_{i=1}^{n} \left[2p_i^2 \frac{\partial B_i}{\partial \lambda} \frac{\partial B_i}{\partial \psi} + 2p_i (p_i B_i + q_i - \theta_i) \frac{\partial^2 B_i}{\partial \lambda \partial \psi} \right]$$ (3-11)

26

Solving equations (3-7) through (3-11) requires the lengthy procedure of taking all first and second partial derivatives of equation (2-16), the expression for angle B. Solutions to these equations are contained in the FORTRAN Fix Program included in this paper.

C. GOLDEN SECTION SEARCH

From equations (2-15) and (3-1), the objective function can be written,

$$\text{Minimize} \quad \sum_{i=1}^{n} (p_i B_i + q_i - \theta_i)^2, \qquad (3-12)$$

the sum of the squared azimuth differences.

Letting x denote the indicated move in longitude and y denote the indicated move in latitude given by equation (3-6),

$$\bar{R} = (\Delta\lambda, \ \Delta\psi)^t$$

$$= (x,y)^t$$

Then angle B_i, given in equation (2-16), becomes at $\bar{P}_{j+1}$

$$B_i = \cos^{-1}\left[\left(\left[\sin(\psi_j - \delta y) \cos\psi_i - \sin\psi_i \cos(\psi_j - \delta y)\right.\right.\right.$$

$$\left[\cos(\lambda_j - \delta x) \cos\lambda_i + \sin(\lambda_j - \delta x) \sin\lambda_i\right]\right) \Big/ \left(\sin\left[\cos^{-1}\right.\right.$$

$$\left(\sin(\psi_j - \delta y) \sin\psi_i + \cos(\psi_j - \delta y) \cos\psi_i \left[\cos(\lambda_j - \delta x)\right.\right.$$

$$\left.\left.\left.\left.\cos\lambda_i + \sin(\lambda_j - \delta x) \sin\lambda_i\right]\right]\right)\right] \qquad (3-13)$$

where subscript j denotes test point coordinates and subscript i denotes DF site coordinates. Since test point

27

coordinates are arbitrarily known and DF site coordinates
are constant for the problem, the substitution of equation
(3-13) into equation (3-12), the objective function, results
in the problem of minimizing a function with a single unknown,
δ, the scalar coefficient.

$$\text{Minimize } f(\delta) = \sum_{i=1}^{n} \omega_i^2(\delta) \qquad (3\text{-}14)$$

The objective function could be evaluated at incremental
values of δ, say over the interval (a,b). Then that δ which
yields the smallest functional value would be chosen as the
scalar coefficient to adjust the move indicated by the
second-order gradient search. The Golden Section Search
(reference 1) provides a fast and methodical approach to find
this minimizing δ. Figure 6 illustrates the problem; however,
the actual curve representing $f(\delta)$ is unknown at the outset
of the problem.

Reducing the Search Interval
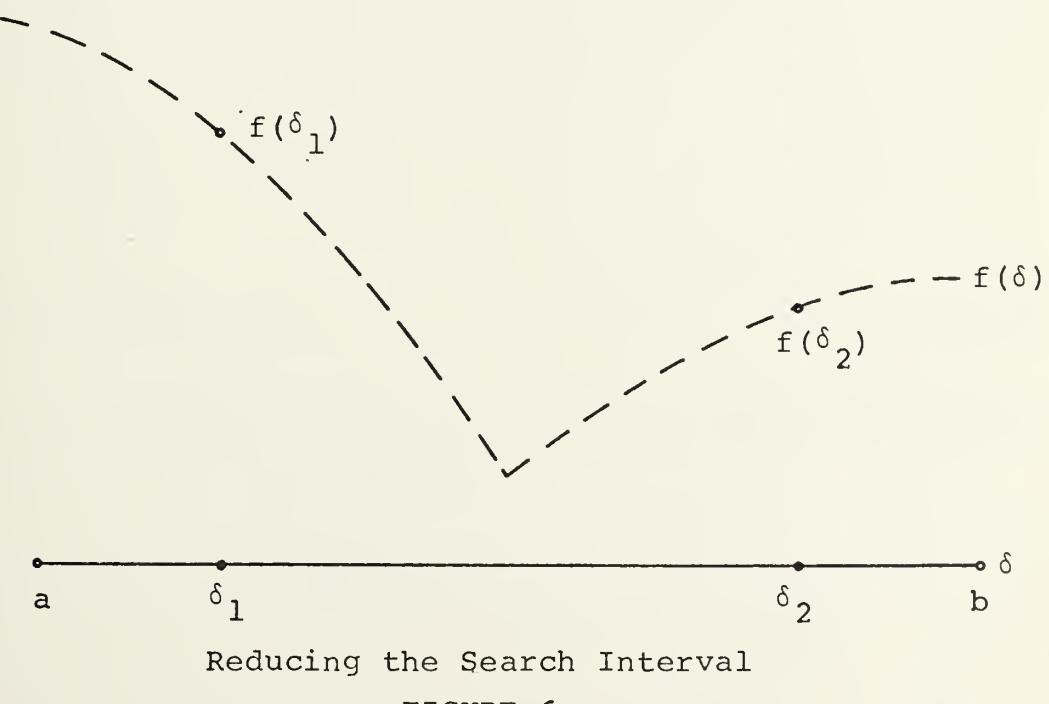
FIGURE 6

Based on the assumption that $f(\delta)$ has a local minimum on (a,b), the objective is to find that minimum without evaluating the function at too many points in (a,b). The Golden Section Search systematically eliminates portions of the interval by comparing functional values of pairs of points in (a,b). From Figure 6, $f(\delta_2)$ is less than $f(\delta_1)$; therefore, the portion (a,δ_1) can be eliminated in searching for the minimum, reducing the search interval to (δ_1,b). A new point then is selected for comparison with $f(\delta_2)$, resulting in a second elimination of whichever end interval corresponds to the higher functional value.

Letting I_n represent the length of the nth search interval,

$$I_1 = b - a$$

Two different values of δ are tested at each trial. By letting the two values be symmetric on I_n, the length of I_{n+1} is the same regardless of which end interval is dropped. Letting σ denote the relative position of δ_1 in I_1,

$$\sigma = (\delta_1 - a)/(b - a)$$

Then

$$\delta_1 = \sigma(b - a) + a \qquad\qquad (3-15)$$

Since δ_2 is symmetric with δ_1, the relative position of δ_2 in I_1 is given by $(1 - \sigma)$, so that

$$1 - \sigma = (\delta_2 - a)/(b - a),$$

and

$$\delta_2 = (1 - \sigma)(b - a) + a \tag{3-16}$$

Provided that δ_2 yielded the minimum functional value, as in Figure 6, then δ_2 becomes the first element of the symmetric pair in I_2 and its relative position in I_2 is given by

$$\sigma = (\delta_2 - \delta_1)/(1 - \sigma)(b - a)$$

$$= \left[(1 - \sigma)(b - a) + a - \delta_1\right]/(1 - \sigma)(b - a)$$

from equation (3-16), so that

$$\delta_1 = (1 - \sigma)^2(b - a) + a \tag{3-17}$$

From equations (3-15) and (3-17), it follows that

$$\sigma(b - a) + a = (1 - \sigma)^2(b - a) + a$$

$$\sigma = (1 - \sigma)^2 \tag{3-18}$$

If, on the other hand, δ_1 yields the minimum functional value, then δ_1 becomes the second element of the symmetric test pair in I_2, and its relative position in I_2 is given by

$$1 - \sigma = (\delta_1 - a)/(1 - \sigma)(b - a)$$

So that

$$\delta_1 = (1 - \sigma)^2(b - a) + a,$$

as in equation (3-17), and leading to the same result as in equation (3-18).

From equation (3-18)

$$\sigma^2 - 3\sigma + 1 = 0$$

which can be solved by the quadratic formula, so that

30

$$\sigma = \left[3 \pm (9 - 4)^{\frac{1}{2}}\right]/2$$

$$= 0.382$$

Substituting this result in equations (3-15) and (3-16),

$$\delta_1 = 0.382 \, (b - a) + a \qquad\qquad (3-19)$$

$$\delta_2 = 0.618 \, (b - a) + a \qquad\qquad (3-20)$$

Generalizing, let b_n and a_n represent the endpoints of the nth search interval. Then

$$\delta_1 = 0.382 \, (b_n - a_n) + a_n \qquad\qquad (3-21)$$

$$\delta_2 = 0.618 \, (b_n - a_n) + a_n \qquad\qquad (3-22)$$

After the first comparison on I_1, either δ_1 or δ_2 is the survivor from the preceding iteration, so that a comparison can be made after evaluating only the new test point symmetric with the survivor. The Golden Section Search terminates when $b_n - a_n < \varepsilon$, where ε may be tailored to the magnitude of the indicated move.

The value of δ which minimizes $f(\delta)$ over (a_1, b_1) is entered in equation (3-6), resulting in a new test point

$$\bar{P}_{j+1} = (\lambda_j, \, \psi_j)^t + \delta \, (x,y)^t \qquad\qquad (3-23)$$

$$= \bar{P}_j + \delta\bar{R}$$

D. FORTRAN FIX PROGRAM

The equations presented in this paper were coded in FORTRAN. The resulting program has been successfully

31

executed on an IBM 360/67 computer system in the W. R. Church
Computer Center at the Naval Postgraduate School.

1. Program Description

The program contains an identification number, longi-
tude, latitude and name for each DF site in an imaginary
network. Inputs to the program are DF site identification
number and signal azimuth. After DF site names and coordi-
nates are correlated with input site identification numbers,
necessary trigonometric functions of site coordinates are
computed and stored in an array. Searching for the minimum
sum of azimuth differences begins from (0,0) with a Golden
Section Search on longitude using (360,0) as the indicated
move. The result is a minimizing longitude on the equator
from which a Golden Section Search is conducted on geocentric
latitude with indicated move (0,180). From this minimizing
geocentric latitude, another Golden Section Search is con-
ducted on longitude with (180,0) as the indicated move.
Such alternating searches on longitude and geocentric lati-
tude continue until diminishing returns are indicated by a
new position being less than 500 nautical miles from the
previous minimizing position. The initial interval for the
Golden Section Search is set at (-1,1), the endpoints for
equations (3-19) and (3-20). Subsequent endpoints are
modified by the search results, producing values for equa-
tions (3-21) and (3-22).

The program then executes second-order gradient
searches refined by Golden Section Searches on indicated

32

moves until the most recent move is less than some input termination value, say one-tenth of a nautical mile. Indicated moves, given by equation (3-6), are unbounded and might occasionally go off the coordinate system of Figure 1. Scaling any such wild moves to the coordinate system by modulo arithmetic destroys both the direction and magnitude of the vector. The indicated moves are kept in bounds by conversion to a unit vector in radians until such moves are of magnitude less than 30 nautical miles, such a small step indicating that the solution is at hand. By converting the indicated move to a unit vector prior to refinement by a scalar coefficient from the Golden Section Search, moves from the second-order gradient search are limited to about 3440 nautical miles per iteration.

Search output on successive iterations is optional, depending on an operator entry. Unless search progress is requested, searching terminates after thirty iterations even if the latest step is greater than the input termination value. After every tenth second-order gradient search, if such a high number should be required, the search effort is jolted by conducting alternate Golden Section Searches on longitude with indicated move (90,0) and latitude with indicated move (0,90). Such Golden Section Search interruptions only yield a new test point when they reduce the current value of the objective function.

Prior to solution output, geocentric latitude is converted to geographical latitude using equation (2-6), and

33

the solution is given in degrees and minutes of longitude, east or west, and latitude, north or south.

2. Results

The program has worked successfully in over ten thousand runs against simulated targets spread randomly over the globe with various networks of DF sites and various numbers of sites intercepting a given target. In actual practice, prior information about a target's area of opera- tion might produce a better starting point than (0,0); how- ever, the time required to type such starting coordinates on a keyboard for input would exceed the total time required for the solution starting from (0,0), which averages less than a second and includes some diagnostic output useful in analyzing results. Figure 7 illustrates a representative set of search iterations with Golden Section Searches plotted as dashed lines and second-order gradient searches solid.
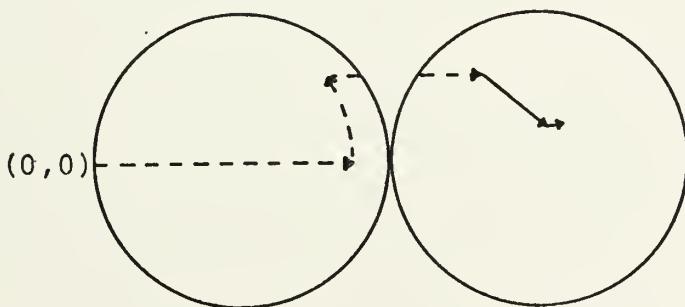
Searching

FIGURE 7

34

IV.   TARGET LOCATION CONFIDENCE REGION

That location yielding the minimum sum of squared azimuth differences, or least squares solution, would coincide with the location of the signal emitter if all measured signal azimuths with respect to the DF sites were free from error. Since then all great circle arcs corresponding to signal azimuths would intersect at a point, the minimum value of the objective function would be equal to zero, as is always the case when only two signal azimuths are available to compute a fix. Because the sites in a DF network do not produce errorless measurements, solutions rarely coincide with the emitter location, and there is the question of how close the emitter might be to the least squares solution.

A.   SIGNAL AZIMUTH ERROR DISTRIBUTIONS

Supposing that signal azimuth measurements made at individual DF sites are not biased in any of the possible directions, then it follows that signed errors have a mean value of zero. If such measurements were found to be biased in certain directions during routine calibration trials, then the amount of bias could be applied as a correction to subsequent measurements, producing an estimated mean value of zero. Lacking any reason to assume a different distribution and following the lead given in the literature of direction finding, the error distribution can be taken to

35

be normally distributed with mean zero and variance σ_i^2, assumed known and independent from site to site.

The error distribution can be made to be symmetric around zero by following the sign convertion that clockwise errors are negative and counter-clockwise errors are positive in sign.

B. THE OBJECTIVE FUNCTION VALUE AS A CHI-SQUARE STATISTIC

From standard textbooks on probability theory (for example, reference 2), it can be verified that if a random variable is normally distributed with mean zero and variance σ^2, then the square of that random variable is governed by the Gamma distribution with parameters $(1/2, 1/2\sigma^2)$. Furthermore, the sum of n independent Gamma distributed random variables divided by the variance of the underlying normal distributions is a Chi-Square statistic with n degrees of freedom. Hence, where ω denotes the azimuth difference,

$$\omega_i \sim N(0, \sigma_i^2) \tag{4-1}$$

$$\omega_i^2 \sim \Gamma\left(\frac{1}{2}, \frac{1}{2\sigma_i^2}\right) \tag{4-2}$$

$$\sum_{i=1}^{n} \frac{1}{\sigma_i^2} \omega_i^2 \sim \chi_{(n)}^2 \tag{4-3}$$

Since the normal distribution here referred to applies to the azimuth differences between the measured signal azimuth and the azimuth of the unknown emitter location, the ω_i refer to actual and unknown errors rather than calculated differences between solution azimuths and signal azimuths.

36

Equation (4-3) therefore specifies the distribution of values of the objective function (equation (3-12)) at unknown emitter locations under the assumption that azimuth errors are normally distributed with known variance.

C. CONFIDENCE LEVELS AND REGION BOUNDARIES

Since the sum of squared azimuth errors divided by variances is a Chi-Square statistic under the previous assumptions, there is a specific probability, denoted α, that this sum will be less than or equal to any given value. Equivalently, for a fixed probability α, or confidence level, there corresponds an upper bound, denoted $C_{(n,\alpha)}$, which depends upon the degrees of freedom as well as the confidence level.

$$P\left(\sum_{i=1}^{n} \frac{1}{\sigma_i^2} \omega_i^2 \leq C_{(n,\alpha)}\right) = \alpha \qquad (4-4)$$

The choice of confidence level, α, is arbitrary, The corresponding value for $C_{(n,\alpha)}$ can be found in Chi-Square tables.

For a given fix problem, the value of the sum of least squares, denoted f*, is the minimum possible value of the Chi-Square statistic for the observed signal azimuths. Furthermore, by evaluating the objective function at successive points outward in any direction from the least squares solution, it can be seen that the farther away the point evaluated up to the antipode, the higher the objective function value. The location corresponding to f* can

37

therefore be regarded as a point in a region which contains
all the possible emitter locations for which the value of
the objective function is less than or equal to an upper
bound $C_{(n,\alpha)}$, given the set of observed signal azimuths.
Such a region is bounded by all locations for which the
objective function has a value equal to $C_{(n,\alpha)}$, and it can
be stated that, for the observed signal azimuths, there is a
probability α that the bounded region will contain the
unknown emitter location.

Daniels and Vajda (1951) challenge the utility of such
an approach on the grounds that at given confidence levels
the corresponding region may not exist with positive
probability if n is greater than two. Their observation is
a consequence of the fact that except for n equal to two
all of the great circle arcs corresponding to signal azimuths
seldom intersect at a single point thereby yielding f*
equal to zero.

Prior to the availability of the high-speed digital
computer, the practical problems of producing such a region
were certainly more striking than theoretical objections.
Even so, the Daniels/Vajda criticism was more than casual,
which may indicate a requirement for additional arguments
to justify the use of such a confidence region.

Suppose that f* is equal to k for some least squares
solution, where

$$P \left(\sum_{i=1}^{n} \frac{1}{\sigma_i^2} \omega_i^2 \leq k \right) = p, \qquad (4-5)$$

38

and the probability p may be determined by interpolating with the value k in a table of Chi-Squared values. Daniels and Vajda are concerned that if the confidence level α had been initially specified at some value less than p, then there exists no region of locations having objective function values less than or equal to k, k being the minimum possible value on the globe for the given signal azimuth observations. There are at least two responses to such an occurrence and the accompanying empty region objection: (1) Increase the confidence level whenever the region does not exist at the prior confidence level so that $C_{(n,\alpha)}$ is greater than k, and (2) Routinely specify a confidence level of sufficient magnitude to make the occurrence of an empty region highly improbable.

Either of the above alternatives insures the production of a non-empty confidence region. There remains the question of what is represented by a possible contention inferable from equation (4-5), namely that positive probability p is attached to a single point, the least squares solution. Any such statement would be puzzling when approached with the viewpoint that specific random variables on a continuum have zero probability and that probability statements can only be made about boundaries for continuous random variables such as location coordinates.

An answer may be attempted by first pointing out that azimuth errors are unknown and independent random variables, but they are attached to actual and unknown emitter azimuths

with respect to the set of intercepting DF sites. Observed signal azimuths have two components, the first of which, emitter azimuth, is dependent upon emitter location. The second component, azimuth error, is independent from site to site and is the theoretical basis for the Chi-Square contour confidence region. Prior to the production of a particular confidence region, the normality assumption permits the specification of upper bounds for the Chi-Square statistic corresponding to various levels of confidence. During production of the particular confidence region, the requirement that a single location must satisfy the observations places a lower bound on the Chi-Square statistic.

Each emitter azimuth can depart from the observed signal azimuth, but there are conceptual bands (based on the error distribution assumptions) bounding such departures for any given probability. When more than two such bands are overlapped in the solution region, then a proportion of the possible combinations of such departures are ruled out by the constraint that azimuth errors are attached to emitter azimuths. Whenever f^* is greater than zero, then the probability, denoted p^*, associated with f^* as an upper boundary from equation (4-5) represents the proportion of impossible sums of squares out of those permitted by the density functions governing azimuth errors.

A thought experiment may clarify these remarks. Suppose it were possible to specify all combinations of azimuth errors permitted by their respective density functions prior

40

to finding the least squares solution. There exists a location satisfying one of the postulated combinations of azimuth errors for a specific set of signal azimuths only if application of each of the postulated azimuth errors in the combination to its corresponding signal azimuth yields a corrected set of emitter azimuths whose corresponding great circle arcs intersect at a point. Few such postulated combinations in the infinite set can be satisfied since the point of intersection for any two corrected emitter azimuths uniquely determines the required azimuth corrections for the rest of the observations. Furthermore, there cannot exist a satisfying location for any postulated combination of azimuth errors having a sum of squares less than f* since no such corrections are of sufficient magnitude to result in a common intersection.

These suggestions can be illustrated by an extreme and improbable example of emptiness of the confidence region for three signal azimuth great circle arcs forming a cocked hat. Suppose that the relationships between the DF sites and the emitter are as given in Figure 8, and suppose that the errors associated with the three DF sites are all governed by the standard normal distribution (variance equal to one degree squared). Suppose also that each of the three signal azimuths were in error by minus two degrees (where the probability that azimuth error is less than or equal to minus two degrees is equal to .0227) in order to form one of the two largest possible cocked hats for $|\omega_i|$ equal to two degrees. Then the least squares solution will be found

41
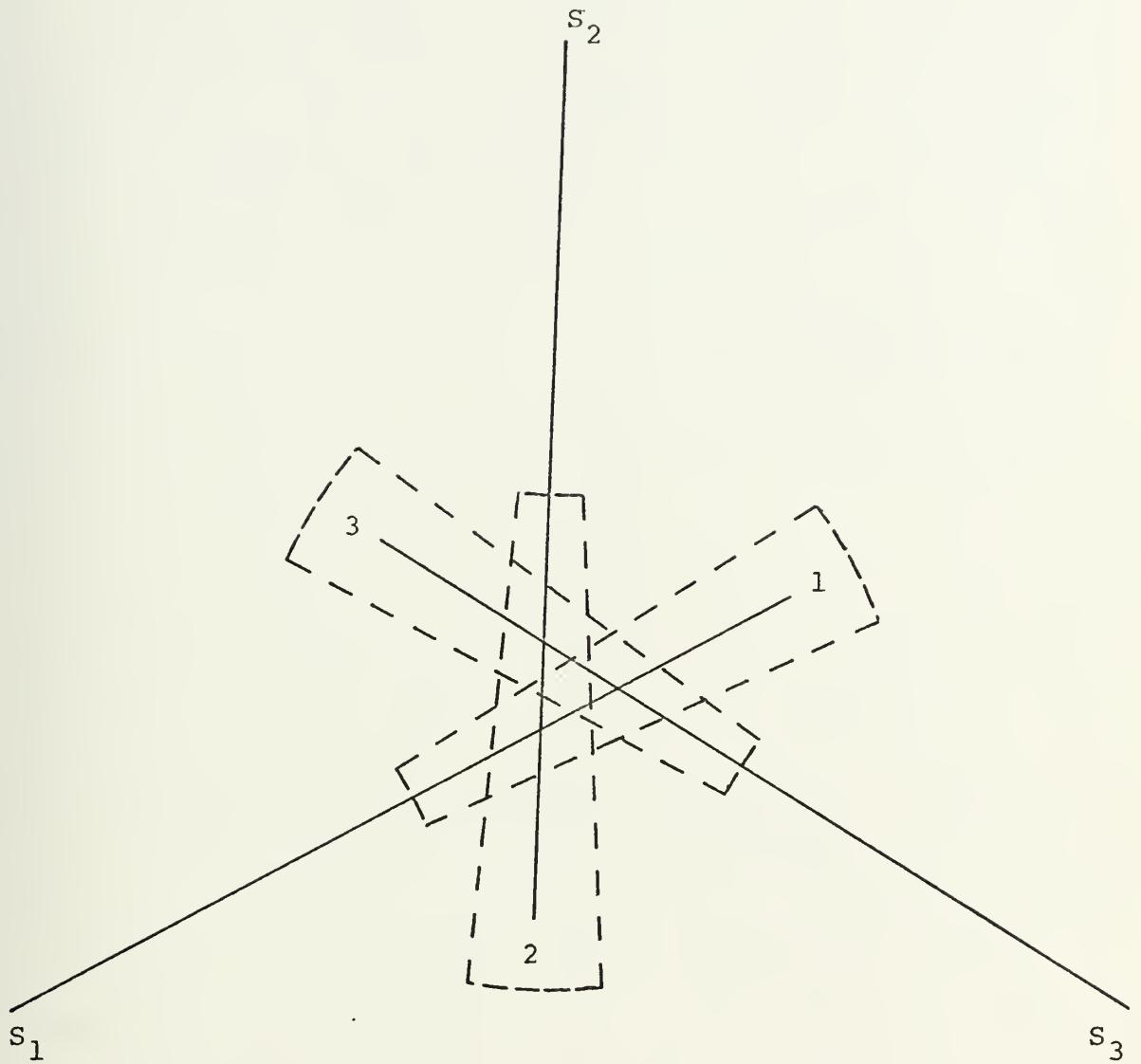
Bounded Signal Azimuths

FIGURE 8

near the center of the cocked hat, and f* is about equal to twelve degrees squared. For three degrees of freedom, there was a .992 probability that the Chi-Square statistic would be less than or equal to twelve degrees squared, indicating an empty confidence region at the .992 level (or any lower levels). Now the probability that $|\omega_i|$ is greater than four degrees is equal to .000, suggesting that a boundary of four degrees on either side of each signal azimuth great circle arc should contain all possible emitter azimuths from which each signal azimuth represents a departure. The situation is illustrated in Figure 8.

With each emitter azimuth free to be anywhere within its dashed band by the normality assumption, but dependent upon the actual emitter location and therefore constrained by the other dashed bands, the shaded intersection of the three bands must (for any non-negligible probability) contain the emitter. Moreover, the Chi-Square contour methodology would produce a circular confidence region within the shaded triangle for any confidence level greater than .992. The center of the shaded region corresponds to the least squares solution. Suppose a "center" to be the least squares solution united with all points forming a neighborhood within radius ε of the center. Then this "center" had a probability of .992 + f(ε) of containing the emitter location. Thus there was a probability of .008 - f(ε) of finding the emitter within a region bounded by a "centerless" circle inscribed in the shaded triangle. There is zero probability that the

43

emitter lies outside such an inscribed circle, or confidence region at the 100 percent level. The description of the confidence region as circular applies to Figure 8 only because the DF sites are equidistant and symmetric around the emitter, and because azimuth errors are minus two degrees.

The implication of the foregoing is that if errors are normally distributed with known variance, then abnormally large cocked hats would be indicative of excellent solutions via the least squares approach. The point would be difficult for operators to accept since high confidence is normally associated with a set of great circle arcs corresponding to signal azimuths that nearly intersect at a point, and large departures are suspect. The discrepancy between the above conclusion and experience may be attributed to the fact that abnormally large cocked hats only occur when outliers (signal azimuth errors that do not obey the empirically estimated distribution) enter the data base.

Sometimes strange relationships between the sizes of cocked hats and accuracy of locations (least squares solutions) can also be demonstrated with a network of three DF sites with errors governed by a Bernoulli distribution, having equal probability that azimuth error is plus or minus three degrees. Figure 9 illustrates the situation. Given an emitter at the center of the star, observed signal azimuths are in error by plus or minus three degrees, each with probability 1/2. All possible configurations of cocked hats are therefore represented on the figure for the
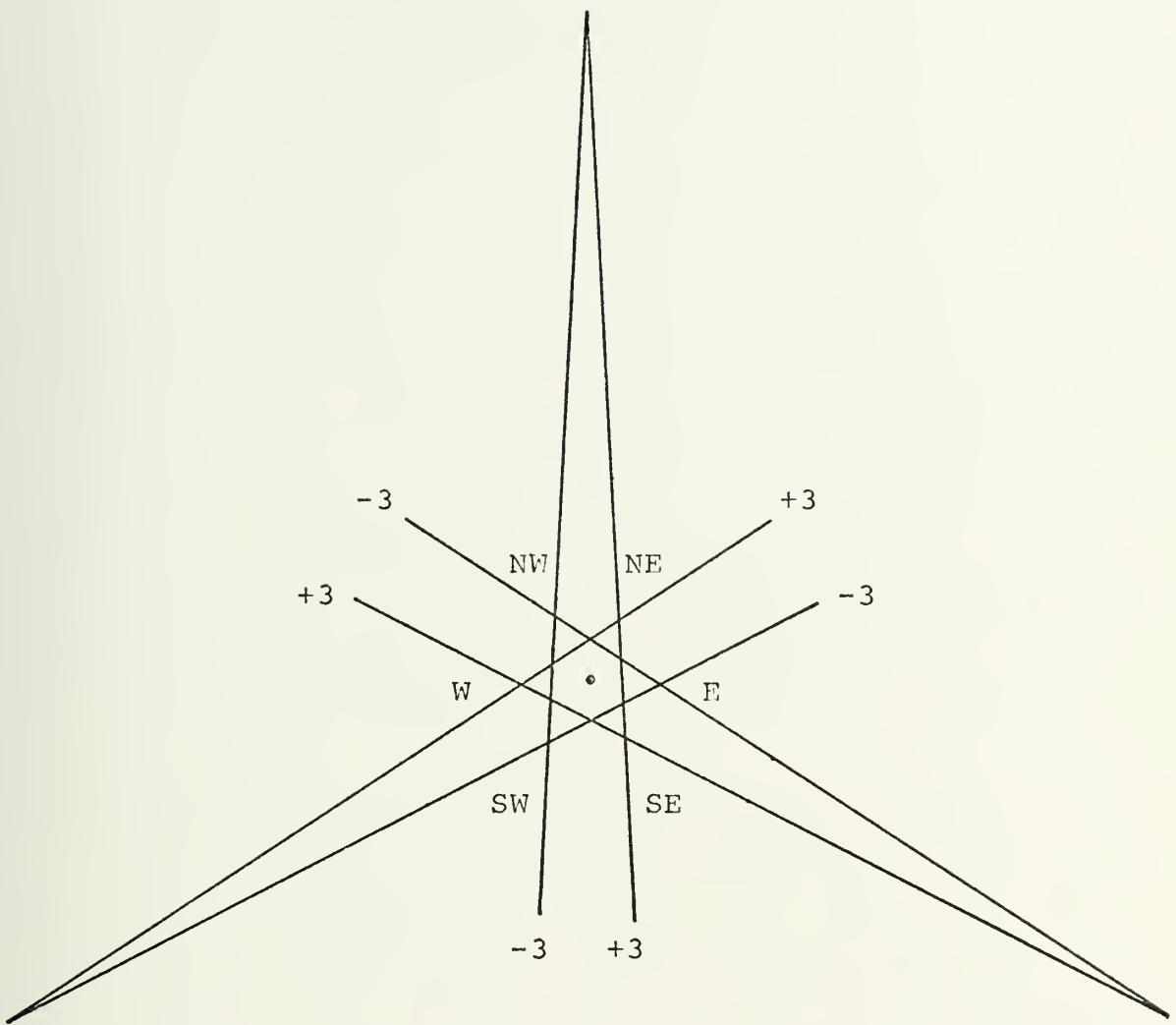
Bernoulli Random Error

FIGURE 9

sketched relationship between DF sites and emitter location. Six of the possible cocked hats are the small triangles at the tips of the star. The other two possibilities are the union of the body of the star with the small triangles at points NE, SE and W, and the union of the body of the star with the small triangles at points E, SW and NW. The latter two cocked hats are abnormally large and have f* equal to 27 degrees squared (which is over twice the value of a Chi-Square statistic at the .995 level for a normal error distribution). Yet, the center of these largest cocked hats coincides approximately with the emitter location, indicating excellent least squares solutions, and the centers of the triangles at the points of the star, the smaller cocked hats, are far from the emitter location, even though their f* value is relatively small.

The probability of occurrence of such large cocked hats when error is governed by a normal rather than Bernoulli distribution is negligible, and they do not appear when data is simulated with a normal error distribution having reasonable variance. However, in about 400 simulations during development of the Fix Program they were forced to appear by governing error with such a Bernoulli distribution. As would be expected from Figure 9, a plot of location error versus f* verified that location error decreases as f* approaches its maximum of 27 degrees squared for this unusual error distribution. Such a simulation naturally yields about 25 percent of the abnormally large cocked hats and 75 per-

46

cent triangles at the points of the star. With a random

distribution of DF sites and signal emitters over the globe,

the stars are not so well-shaped as that in Figure 9.

If one regards the fix problem with least squares solu-

tion and confidence region construction at confidence level

α as a Bernoulli trial with success if the confidence region

contains the emitter location and failure if the emitter is

outside the confidence region, then the expected number of

successes for m independent trials is αm. That the Chi-

Square contour confidence regions have normalized frequency

of containment about equal to the probability of containment

is therefore expected to be true and was demonstrated to be

true by simulation. At confidence level α, on about α per-

cent of the trials non-empty confidence regions are produced

which contain the actual emitter. On the remaining (1 - α)

percent of the trials, outcomes are distributed among empty

regions and non-empty regions with the actual emitter out-

side the confidence region. The lower the confidence level

the higher the proportion of empty regions among the failures.

D. FORTRAN CONFIDENCE REGION PROGRAM

A plot subroutine is included in the Fix Program of this

paper. Sample plots are included in the Computer Output

section of the paper. The plot is a square grid of constant

dimension, scaled in nautical miles to contain the confidence

region. An asterisk on the grid indicates that the corres-

ponding point has an objective function value greater than

the Chi-Square boundary value for the specified confidence

47

level. The least squares solution is at the center of the grid and is indicated by the letter S. During program development, it was found that a 90 percent confidence level is sufficient to preclude the occurrence of empty confidence regions, and the sample regions are of that size.

1. Program Description

Given in a data statement of the subroutine are Chi-Square values corresponding to the numbers of possible degrees of freedom, up to n for a network of n DF sites, and the selected confidence level. The confidence region boundary value is selected according to the number of signal azimuths available to find a solution.

The dimension of the grid is 41 rows and 51 columns, tailored to the line printer distances between rows and columns, so that the ratio of the distances between rows and columns is 4:5. Depending upon the scale of the grid, coordinates on the globe are calculated to match each of the 2091 points on the grid. Curvature of the earth calculations are used to determine distances between points on the grid, thereby avoiding distortion inherent in planar assumptions.

At each of the points on a row, the sum of squared azimuth differences is computed for comparison with $C_{(n,\alpha)}$, an asterisk being assigned for grid entry if $C_{(n,\alpha)}$ is exceeded. After the confidence region is exited on a given row, remaining points on the row are assigned asterisks without computation. Similarly, after the confidence region

48

is completed, the rest of the grid is filled with asterisks
without computation.

The area of the confidence region is estimated by
counting the blanks and multiplying their sum by the area
represented by each cell, 80 square miles in the case of
a 400 by 400 nautical mile grid. If computations on the
first row yield any points with objective function value less
than or equal to $C_{(n, \alpha)}$, then the grid is rescaled to cover
a greater area, and the computation starts over. If the
confidence region leaks out on either of the sides of the
grid during computation, then again the grid is rescaled,
and computation starts over. In practice, the initial area
covered by the grid can be tailored to the network and
expected size of confidence regions.

2. Results

If the solution search in the Fix Program should
terminate in the region of the least squares solution before
the least squares point is found, then the confidence region
is noticeably asymmetric about the center at S. The lack of
symmetry indicates that the fix solution should be recomputed
with a smaller termination step. The center of the confi-
dence region, or least squares location, could also be
estimated from the grid itself, but only to an accuracy
limited by the dimensions of a cell.

The confidence region subroutine was used successfully
in over a thousand runs with simulated data. Its chief
deficiency is the computer time required to produce the grid

entries, averaging slightly over ten seconds for numbers of
signal azimuths per target varying uniformly from three to
nine. On a slower machine than the IBM 360/67, the subrou-
tine would require revision to be usable for production.
Sampling every other or every third cell would be possible
avenues for reducing computation time, but the present
version was preferred for a more accurate estimate of con-
fidence region area. A more sophisticated method for reduc-
ing computation time would be to use a modified Golden
Section Search to find the confidence region boundary outward
from the center of the region, store coordinate pairs of the
boundary in an m by n array, and then print the boundary on
a scaled grid.

V. INTERCEPT GEOMETRY

The Fix Program produces several statistics that are
useful in describing intercept geometry. The first group
of these statistics is related to signal azimuths and is
used to plot position lines as linear approximations of the
great circle arcs in the region of the solution. In the
second group are some values to which location error is
sensitive.

A. PLOTTING POSITION LINES IN SOLUTION REGION

Following the optional summary of search progress, the
least squares solution and the value of f*, the computer
output has a table of values in which each row corresponds
to one of the intercepting DF sites. Row entries include
the site identification number, the site name, the azimuth
of the solution, the signal azimuth, their difference, the
range in nautical miles from the solution to the site, and
three values used to plot the position line relative to the
least squares solution. These values are calculated by
analogy with a right spherical triangle illustrated in
Figure 10.

Figure 10 is labelled to correspond to the base of the
polar triangle of Figure 3 with the DF site at vertex B and
the least squares solution at Vertex C. Vertex angle A is
a right angle formed by connecting C to the closest point of
approach (CPA) of the great circle arc related to the signal

51
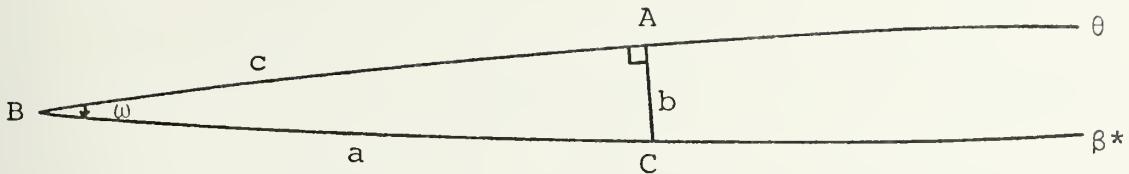
Right Spherical Triangle

FIGURE 10

azimuth θ. Arc a, connecting the DF site and least squares
solution, is related to the solution azimuth, denoted β^*,
and is given by equation (2-11), using the polar triangle of
Figure 3. By the law of sines for spherical triangles,

$$\sin b = \sin\omega \sin a \qquad (5-1)$$

The curvature of earth distance covered by arc b is
closely approximated by multiplying arc b in radians by the
mean earth radius of 3439.9 nautical miles, yielding the
nautical mile departure of the CPA from the solution.

The site azimuth with respect to the solution, denoted
γ^*, is found after calculating angle C of Figure 3 in the
same manner that vertex angle B and azimuth β were calculated
in equations (2-12) and (2-13). Then the azimuth of the CPA
with respect to the solution is the sum of γ^* and C, in the
case illustrated. Finally, the azimuth of the DF site with
respect to the CPA is found by subtracting 90 degrees from
the sum of γ^* and C, in the case illustrated. Similar argu-
ments apply to three other general cases, solution east or
west of the DF site and ω positive or negative, and resulting
conditional equations are included in the Fix Program.

The azimuth and distance of the CPA with respect to the solution are the components of a vector which can be plotted on polar coordinate paper. A line of position perpendicular to this vector approximates the great circle arc in the region of the solution. The direction of the intercepting DF site is given by the azimuth value in the last column of the output row. The plot can also be constructed with a parallel ruler by orienting the ruler along the site azimuth with respect to the CPA, moving the free edge the distance to scale of the CPA toward the azimuth of the CPA. Such lines of position are plotted to the grid scale on several of the confidence region plots provided in the computer output section of this paper.

B. MEAN ACUTE ANGLE OF INTERSECTION

There are factors that may be said to reduce location error, given that signal azimuth error is present but unknown. One such factor is the number of DF sites providing signal azimuths to make a fix: the more independent measurements, the better the emitter location estimate by least squares solution. Another factor is the layout of the DF network, the obvious supposition being that a network spread over a large area produces better locations of globally distributed targets than a network confined to a small area.

A slightly less obvious statistic is the magnitude of the acute angle of intersection of great circle arcs corresponding to signal azimuths. For two DF sites participating, the dependence of location error on the acute angle of

53

intersection is illustrated in Figure 11. In case a, two
lines of position intersect at about 90 degrees; in case b,
the acute angle of intersection is about ten degrees. The
difference in the sizes of regions contained by the dashed
lines demonstrates the effect of two degree uncertainty of
measurement on either side of a signal azimuth on the two
different intersections.

Although the confidence regions described in Section IV
of this paper do convey this dependence, that for case a
being a near circle contained in the dashed lines and that
for case b being an elongated ellipse of orientation and
dimension similar to to the dashed region, the acute angle
of intersection statistic was found to be significant enough
to warrant isolated analysis. It can be demonstrated
graphically that the dependence also exists for n greater
than two. For all cases, the dependence can be examined by
calculating the mean value of all the acute angles of inter-
section formed by all possible permutations of two lines of
position, given by $(n)_2$. The mean acute angle of inter-
section is part of the Fix Program output. Dependence of
location error on this statistic is examined in later sec-
tions of this paper. For individual pairs, the acute angle
of intersection is closely approximated by taking differences
from the site azimuths with respect to the CPA.
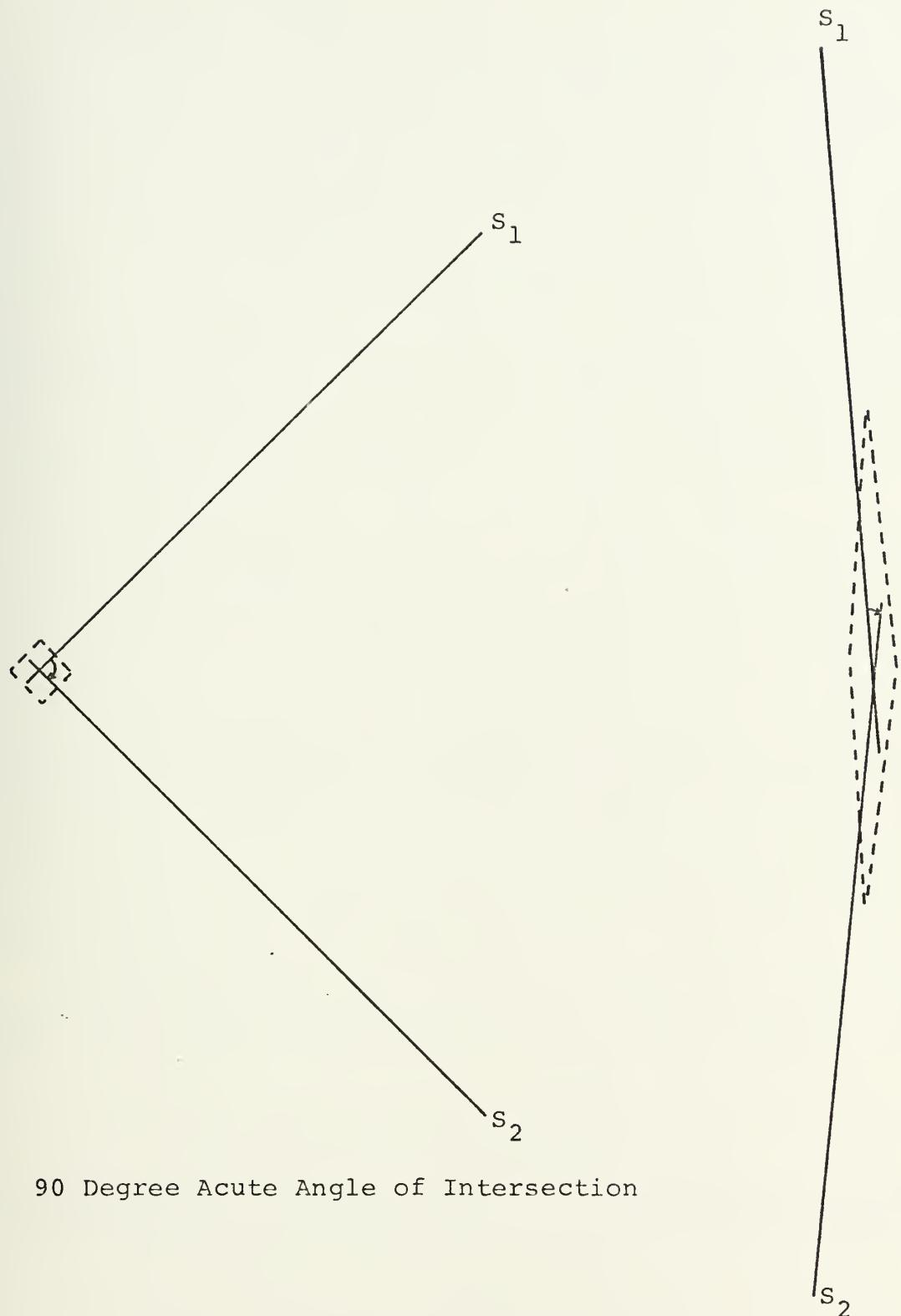
a.   90 Degree Acute Angle of Intersection

b.   10 Degree Acute Angle of Intersection

FIGURE 11

C.   MEAN ARC STATISTIC

A more subtle factor affecting location error is a function of arc length or distance from the DF site to the emitter location. The arc from the DF site to the emitter and all other arcs representing possible departures due to erroneous signal azimuth measurements converge at the DF site and at its antipode. Therefore, the maximum nautical mile departure of a line of position from the emitter location for constant azimuth error occurs at 90 degrees of arc, or about 5403 nautical miles, from the DF site.

The arc from the DF site to the least squares solution is given by equation (2-11). The arc statistic is equal to this arc, or to its supplement if the arc is greater than 90 degrees. The dependence of location error on the arc statistic is illustrated in Figure 12, where the solid line represents an arc from the DF site through the emitter location to the DF site antipode, and the dashed lines represent three degree departures from this arc.

The distance from the site-to-emitter arc to the departure arcs increases non-linearly from zero at the DF site

Site   Antipode

Relating Error to Emitter Distance

FIGURE 12

56
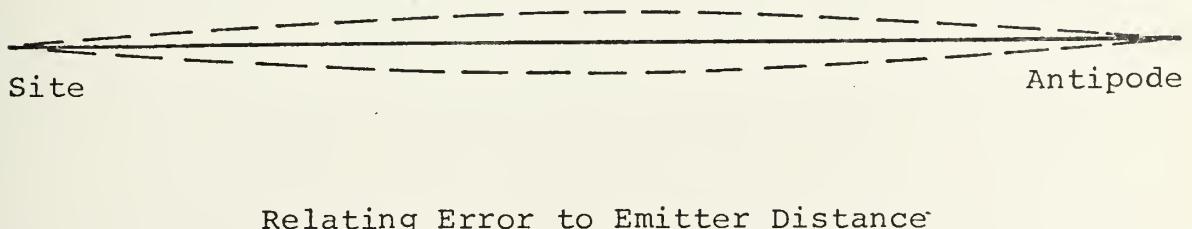
and its antipode to 180 nautical miles at the midway point. In a later section of this paper, location error sensitivity to the mean arc statistic for all DF sites participating in the location is examined.

VI. SIMULATION PROCEDURE

A modified version of the Fix Program was used to simu-
late operation against targets. Targets were generated by
a subroutine which provided longitude and geocentric lati-
tude describing random locations uniformly distributed over
the globe. Such coordinates were saved for later comparison
with the least squares solution.

The number of intercepting sites for each target was
either specified for simulations on fixed degrees of freedom,
or randomly generated according to a uniform distribution
from three to nine. In both cases, the specific intercept-
ing DF sites were randomly selected from a set of 19 DF sites
composing the particular network being simulated. Azimuths
of the target location with respect to the participating DF
sites were then calculated. For each such emitter azimuth,
a random error was added, with direction and magnitude of
the error governed by the standard normal distribution. The
emitter azimuth with error was then treated as a measured
signal azimuth for input with the site identification number
to the Fix Program.

During program development, the simulation procedure was
used with zero signal azimuth error generated to insure that
the least squares solution of the search procedure coincided
with the target coordinates to at least an accuracy of three
decimal places. A search termination value of one-tenth of

a nautical mile was found to be adequate, and the present combination of Golden Section Searches and second-order gradient searches was found to be satisfactory during the development simulations. The Fix Program has also been successfully tested with up to 19 participating DF sites on a single target, with a set of DF sites contained in a 180 by 240 nautical mile area, and with higher variance error distributions, including outliers.

A. GEOCENTRIC AND GEOGRAPHICAL LATITUDE

A comparison of least squares solutions using geocentric and geographical latitude in Fix Program calculations was made in order to examine the accuracy gain of the geocentric model. Errorless signal azimuths of random targets were computed using geocentric latitude in calculations. A least squares solution was then found by using geographical latitude in calculations, and the conversion of the solution to geographical latitude was omitted. This distance between the geographical coordinates of the target and the pseudo-geographical coordinates of the least squares solution measures the departure from the least squares location due to use of geographical latitude on an assumed sphere.

Radial departures for two degrees of freedom were occasionally devastating (424 nautical miles in one case). Using an imaginary network, called the national network, and degrees of freedom uniformly distributed from three to nine, the mean radial departure for 148 samples was 6.8 nautical miles. The direction of such departures tends toward the equator for targets in both northern and southern hemispheres.

59

# VII. LOCATION ERROR ANALYSIS WITH FIXED DEGREES OF FREEDOM

The sensitivity of location error to several factors was examined in simulations with degrees of freedom fixed from two to seven. From 100 to 200 samples were generated at each level for each of the networks. All of the following plots are drawn to the same scale to simplify between plot comparisons of the effects of different degrees of freedom and different network configurations. Values too large for the common scale are entered in a row at the upper limit of the plot above an off of scale indicator.

A. COMPARISON OF ERROR ON NATIONAL AND GLOBAL NETWORKS

Member sites of the national network varied in longitude from Attu to Boston and in latitude from Anchorage to Honolulu. The specific sites are identified in the second data statement of the Fix Program. Sites in the widely distributed global network included Anchorage, Bombay, Boston, Buenos Aires, Cape Town, Christchurch, Dakar, Honolulu, Houston, Lima, Naples, Papeete, Perth, Recife, Seattle, Seychelles, Tehran, Tokyo and Wake.

Figure 13 is a plot of mean location error from each of the sample groups against the number of intercepting sites. Dashed lines connect the means of each network. The plot shows nearly double the location error in the national network even at higher degrees of freedom.

60

FIGURE 13

Location Error Versus
Degrees of Freedom

National

Global
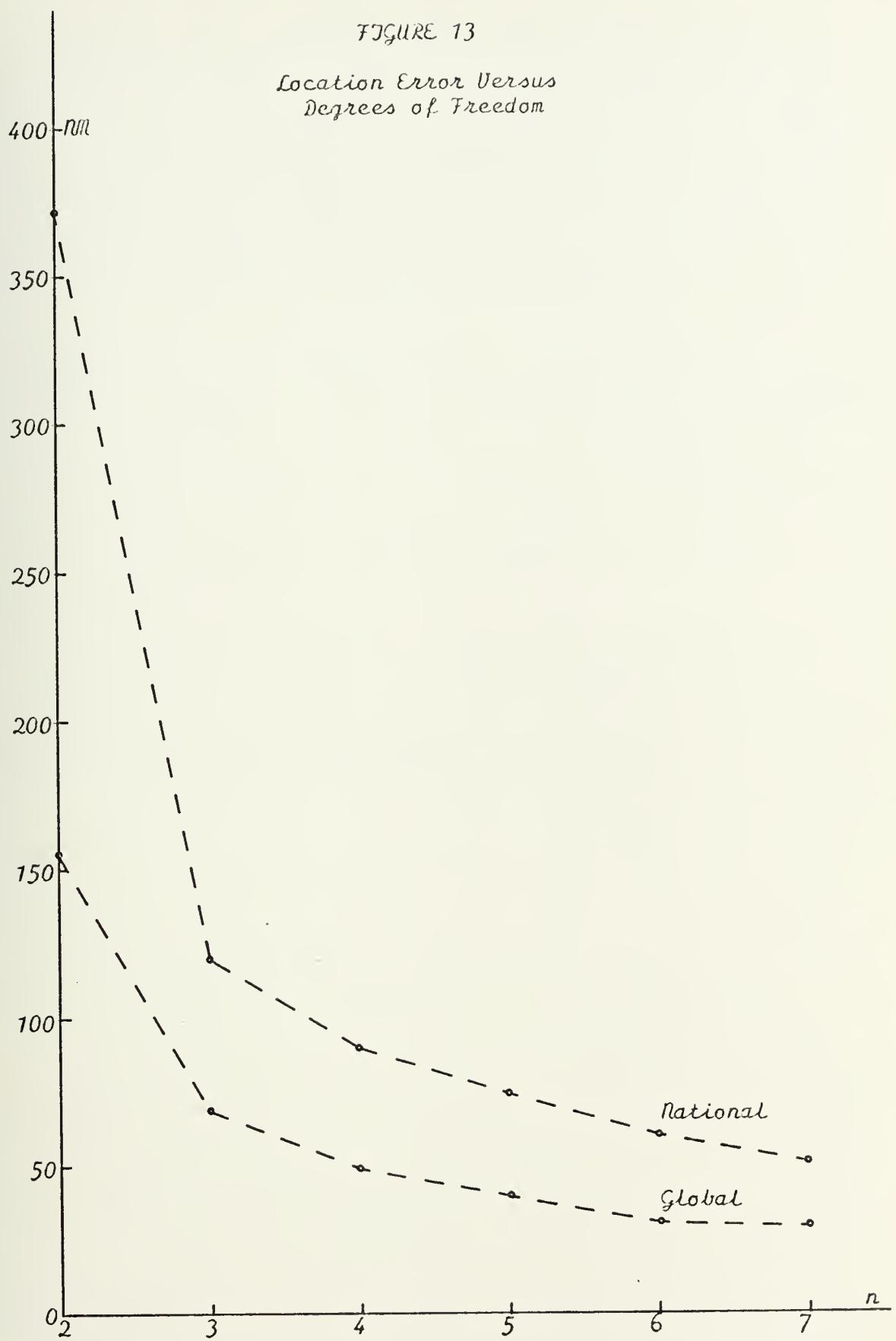
With all other factors random, the average accuracy of a network is dependent upon the network layout and the variance of signal azimuth measurement error. For a given network, the mean location error would vary in the same direction as changes in such variance, in all of the following simulations held constant at one degree.

B. ERROR VERSUS MEAN ACUTE ANGLE OF INTERSECTION

Based on samples from the national network, Figures 14, 15 and 16 are scatter plots of location error versus the mean acute angle of intersection explained in section V-B. Degrees of freedom were fixed at three, five and seven, respectively.

The strong correlation in the national network can be interpreted as a reduction of both the mean and variance of location error as intersections of great circle arcs are less acute. Rough scatter plots for two, four and six degrees of freedom showed the same correlation, naturally most pronounced at two degrees of freedom. The set of plots shows a shrinking of the range of the mean acute angle of intersection statistics as degrees of freedom are increased.

Figures 17, 18 and 19 are similar scatter plots with entries from simulations on the global network. The correlation is still evident at three degrees of freedom but becomes masked at higher levels as the layout of the network reduces the chance of producing a combination of target and intercepting sites with a small mean acute angle of inter-

Scatter plot of location error versus mean acute angle of intersection in national network with three degrees of freedom

FIGURE 14

63

Scatter plot of location error versus mean acute angle of intersection in national network with five degrees of freedom

FIGURE 15

64

Scatter plot of location error versus mean acute angle of intersection in national network with seven degrees of freedom

FIGURE 16

Scatter plot of location error versus
mean acute angle of intersection in
global network with three degrees of
freedom

FIGURE 17

66

Scatter plot of location error versus mean acute angle of intersection in global network with five degrees of freedom

FIGURE 18

67

Scatter plot of location error versus mean acute angle of intersection in global network with seven degrees of freedom

FIGURE 19

68

section. Consequently, shrinking of the range of the statistic is extremely evident on Figures 18 and 19.

C.   ERROR VERSUS MEAN ARC STATISTIC

Figures 20, 21 and 22 are scatter plots of national network location error versus the mean arc statistic (explained in section V.C) for three, five and seven degrees of freedom, respectively. At all levels, the large location errors tend to be associated with the high end of the range of mean arc statistics. The strength of the correlation appears to increase as degrees of freedom increase on successive plots.

Figures 23, 24 and 25 are similar plots for the global network. Again, the correlation is masked after three degrees of freedom with the shrinkage effect extremely pronounced as the degrees of freedom increase.

num

Scatter plot of location error
versus mean arc statistic in
national network with three
degrees of freedom

off of scale

FIGURE 20

Scatter plot of location error versus mean arc statistic in national network with five degrees of freedom

off of scale

FIGURE 21

Scatter plot of location error versus mean arc statistic in national network with seven degrees of freedom

FIGURE 22

72

Scatter plot of location error versus mean arc statistic in global network with three degrees of freedom

off of scale

FIGURE 23

73

Scatter plot of location error versus mean arc statistic in global network with five degrees of freedom

FIGURE 24

Scatter plot of location error versus mean arc statistic in global network with seven degrees of freedom

FIGURE 25

IIX. LOCATION ERROR ANALYSIS WITH VARYING DEGREES OF FREEDOM

Simulations were conducted on both networks with degrees of freedom generated uniformly from three to nine. Chi-square contour confidence regions were generated for each target's least squares solution. Using a confidence level of 90 percent, national network confidence regions contained 90.38 percent of the generated targets. Results for the global network were 90.44 percent. Such close agreement between the confidence level and containment in the simulations is dependent upon a reliable standard normal azimuth error generator. In production use, such reliability could only be achieved by having a good estimate of DF site variances.

A. NATIONAL NETWORK

Figure 26 is a scatter plot of confidence region area versus location error. Again using a common scale to aid network comparison, eleven points off the scale are entered above or to the right of an indicator. Although there is one hopeful cluster near the plot origin, the large variance in location errors at given confidence region areas is indicative of the futility of predicting location error based on the size of this reliable confidence region model.

Figure 27 is a multi-level histogram of location error at the various degrees of freedom, demonstrating the same sort of correlation evident in Figure 13. Figure 28

FIGURE 26

Scatter plot of confidence region area versus location error in national network

Location error versus degrees of freedom in national network

FIGURE 27

78

Scatter plot of location error versus mean acute angle of intersection in national network

FIGURE 28

illustrates the correlation between location error and the mean acute angle of intersection, present even with mixed degrees of freedom. The same holds true in Figure 29, a plot of location error versus the mean arc statistic.

B. GLOBAL NETWORK

Figures 30 through 33 are similar plots for the global network. On Figure 30, location error and confidence region area appear independent. Figure 31 shows good correlation between location error and degrees of freedom. Figures 32 and 33 show nearly complete masking of the previously established correlations due to the layout of the network.

Scatter plot of location error versus mean arc statistic in national network

FIGURE 29

81

Scatter plot of confidence
region area versus location
error in global network

FIGURE 30

82
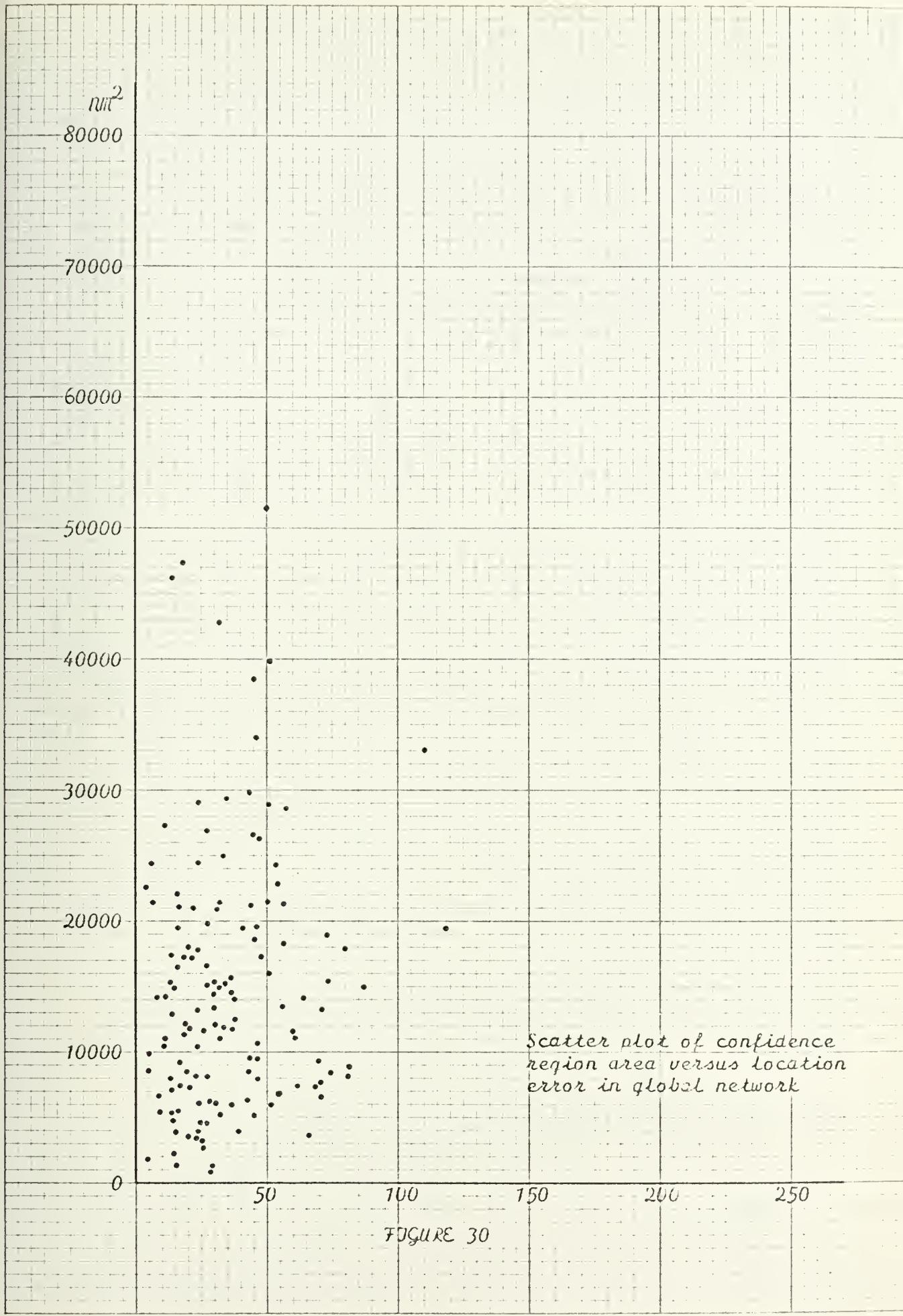
Location error versus degrees of freedom in global network

FIGURE 31

83

Scatter plot of location error versus mean acute angle of intersection in global network

FIGURE 32

Scatter plot of location error versus mean arc statistic in global network.

FIGURE 33

IX. CONCLUSION

The Fix Program and Chi-Square contour confidence region subroutine could be integrated into the software of position location systems by direction finding. The present program (with target and azimuth error generators included) could be used to simulate an existing DF network for accuracy studies on potential targets in different regions of the globe or for studies on optimal placement of DF sites in a proposed network.

The relationships demonstrated in the sections on location error analysis indicate that larger location errors accompany contraction of the network layout; however, this factor would be mitigated by a practice of assigning regional rather than globally distributed targets to the network for prosecution.

Countering the widespread belief that small confidence regions indicate accurate locations and large confidence regions indicate poor locations, it has been demonstrated that for a reliable model location error and confidence region area are nearly independent.

The relationships examined as parts of location error analysis suggest an alternative answer for the question of how accurate is a given location. For an existing network, data could be collected from locations of known transmitters. Such data would include statistics on number of signal

azimuths available to make the fix, mean acute angle of inter-
section and mean arc statistic. With known location error
as the dependent variable, multiple linear regression
analysis could be used to develop regression and correlation
coefficients for predicting location error as a function of
independent variables measured or calculated at the time of
location.

The workability of such an approach was not demonstrated
in the present paper for several reasons: (1) The effort
required to perform the multiple linear regression (using a
standard program from the IBM scientific subroutine package)
would be a project in itself and would be best reserved for
actual data from an existing network. (2) System operators
would be aware of other measurable factors for inclusion as
independent variables in the regression analysis, such as
variance on given signal azimuth measurements, signal
strength and measurement duration.

FIX PROGRAM

```
      REAL LAMBDA,N,NL,NP,NLL,NPP,NPL
      DIMENSION DFSITE(6,19),DOMEGA(19),SYMBOL(4),BETA(19),
     1STAAZ(19)
      COMMON/SITES/SITE(10,19),NUMBER
      COMMON/SIGNAL/THETA(19)
      DATA TWOPI/6.283185/,PI/3.141593/,RADDEG/57.29578/,
     1DEGRAD/1.745329E-2/,FNCECC/1.006768/,SCREEN/.9999999/,
     2PIHALF/1.570796/,SYMBCL/'N','S','E','W'/
      DATA DFSITE/
C     IDENT LONG         LAT      SITE NAME
      1   1.,  210.117,  61.217,'ANCH','ORAG','E    ',
      2   2.,  173.250,  52.933,'ATTU','    ','    ',
      3   3.,  288.933,  42.350,'BOST','ON  ','    ',
      4   4.,  262.600,  27.800,'CORP','US C','HRIS',
      5   5.,  254.983,  39.717,'DENV','ER  ','    ',
      6   6.,  276.950,  42.333,'DETR','OIT ','    ',
      7   7.,  253.517,  31.750,'EL P','ASO ','    ',
      8   8.,  247.983,  46.600,'HELE','NA  ','    ',
      9   9.,  202.133,  21.317,'HONO','LULU','    ',
      1  10.,  241.750,  34.050,'LOS ','ANGE','LES ',
      2  11.,  279.800,  25.767,'MIAM','I   ','    ',
      3  12.,  182.633,  28.217,'MIDW','AY  ','    ',
      4  13.,  266.783,  44.983,'MINN','EAPO','LIS ',
      5  14.,  273.200,  36.150,'NASH','VILL','E   ',
      6  15.,  269.883,  29.967,'NEW ','ORLE','ANS ',
      7  16.,  283.767,  38.667,'NORF','OLK ','    ',
      8  17.,  240.200,  39.517,'RENO','    ','    ',
      9  18.,  237.667,  47.600,'SEAT','TLE ','    ',
      1  19.,  262.667,  37.683,'WICH','ITA ','    '/
      READ (5,1) KILL,CUT
0900  READ (5,1) NUMBER
      IF (NUMBER.EQ.0) GO TO 4200
      WRITE (6,9)
9     FORMAT ('1')
1     FORMAT (I2,F8.3)
      DO 1000 K = 1,NUMBER
      READ (5,1) ID,THETA(K)
      THETA(K)=THETA(K)*DEGRAD
      SITE(1,K)=DFSITE(2,ID)*DEGRAD
      SITE(2,K)=SIN(SITE(1,K))
      SITE(3,K)=COS(SITE(1,K))
      SITE(4,K)=ATAN(0.9932773*TAN(DFSITE(3,ID)*DEGRAD))
      SITE(5,K)=SIN(SITE(4,K))
      SITE(6,K)=COS(SITE(4,K))
      SITE(7,K)=DFSITE(1,ID)
      SITE(8,K)=DFSITE(4,ID)
      SITE(9,K)=DFSITE(5,ID)
1000  SITE(10,K)=DFSITE(6,ID)
C PERFORM ALTERNATING GOLDEN SECTION SEARCHES CN LONGITUDE
C AND LATITUDE
      PSI=0.
      LAMBDA=0.
      SAVEL=LAMBDA
      SAVEP=PSI
      DEGF=615600.
      DO 1400 J = 1,5
      DIV=J
      X=1./DIV*TWOPI
      Y=0.
      CALL SEARCH(LAMBDA,PSI,X,Y,DEGF)
      IF (KILL.EQ.2) GO TO 1100
      CALL SHIFT(SAVEL,SAVEP,LAMBDA,PSI,1,DEGF,DIST)
1100  CONTINUE
      X=0.
      Y=1./DIV*PI
      CALL SEARCH(LAMBDA,PSI,X,Y,DEGF)
      IF (KILL.EQ.2) GO TO 1200
      CALL SHIFT(SAVEL,SAVEP,LAMBDA,PSI,1,DEGF,DIST)
      GO TO 1300
1200  CALL AZDIST(SAVEL,SAVEP,LAMBDA,PSI,AZGO,DIST)
```

```
           SAVEL=LAMBDA
           SAVEP=PSI
1300       IF (DIST.LE.500.) GO TO 1500
1400       CONTINUE
1500       M=0
1600       M=M+1
           COSLAM=COS(LAMBDA)
           SINLAM=SIN(LAMBDA)
           COSPSI=COS(PSI)
           SINPSI=SIN(PSI)
           FL=0.
           FP=0.
           FLL=0.
           FPP=0.
           FPL=0.
C EVALUATE FIRST AND SECOND PARTIALS OF OBJECTIVE FUNCTION
           DO 2450 K = 1,NUMBER
           A=1.
           C=0.
           UA=SINPSI*SITE(6,K)
           UB=COSPSI*SITE(5,K)
           UC=COSLAM*SITE(3,K)+SINLAM*SITE(2,K)
           UD=-SINLAM*SITE(3,K)+COSLAM*SITE(2,K)
           UE=COSPSI*SITE(6,K)
           UF=SINPSI*SITE(5,K)
           UG=UF+UE*UC
           UH=UB-UA*UC
           UI=-UE*UD
           N=UA-UB*UC
           NL=-UB*UD
           NP=UE+UF*UC
           NLL=UB*UC
           NPP=-N
           NPL=UF*UD
           IF (UG.GE.1.) UG=SCREEN
           IF (UG.LE.-1.) UG=-SCREEN
           D=SIN(ARCOS(UG))
           UJ=1./D
           DL=UJ*UG*UI
           DP=-UJ*UG*UH
           DLL=UJ*(UG*UE*UC+UI*UI-DL*DL)
           DPP=UJ*(UG*UG-UH*UH-DP*DP)
           DPL=UJ*(UG*UA*UD+UH*UI-DP*DL)
           COSB=N*UJ
           IF (COSB.GE.1.) COSB=SCREEN
           IF (COSB.LE.-1.) COSB=-SCREEN
           B=ARCOS(COSB)
           COTB=COTAN(B)
           CSCB=1./SIN(B)
           BL=UJ*(DL*COTB-NL*CSCB)
           BP=UJ*(DP*COTB-NP*CSCB)
           UK=UJ*CSCB
           BLL=UK*(UJ*DL*(NL-DL*COSB)+DLL*COSB-BL*DL*CSCB-NLL+
          1BL*NL*COTB)
           BPP=UK*(UJ*DP*(NP-DP*COSB)+DPP*COSB-BP*DP*CSCB-NPP+
          1BP*NP*COTB)
           BPL=UK*(UJ*DP*(NL-DL*COSB)+DPL*COSB-BP*DL*CSCB-NPL+
          1BP*NL*COTB)
           TEST=SITE(1,K)-LAMBDA
           IF (TEST) 1700,2000,1800
1700       IF (TEST+PI) 1900,2000,2000
1800       IF (TEST-PI) 1900,2000,2000
1900       A=-1.
           C=TWOPI
2000       TEST=A*B+C-THETA(K)
           BETA(K)=(A*B+C)*RADDEG
           IF (ABS(TEST)-PI) 2400,2400,2100
2100       IF (TEST) 2200,2400,2300
2200       C=C+TWOPI
           GO TO 2400
2300       C=C-TWOPI
2400       OMEGA=A*B+C-THETA(K)
```

89

```
            DCMEGA(K)=OMEGA*RADDEG
            UL=2.*A*(A*B+C-THETA(K))
            FL=FL+UL*BL
            FP=FP+UL*BP
            FLL=FLL+2.*BL*BL+UL*BLL
            FPP=FPP+2.*BP*BP+UL*BPP
            FPL=FPL+2.*BP*BL+UL*BPL
2450        CONTINUE
            UM=1./(FLL*FPP-FPL*FPL)
            X=(FPL*FP-FPP*FL)*UM
            Y=(FPL*FL-FLL*FP)*UM
C IF EITHER X OR Y ARE GREATER THAN PI AND UNTIL WITHIN 30
C NM OF THE INDICATED MOVE, CONVERT (X,Y) TO A RADIAN UNIT
C VECTOR
            IF (AMAX1(X,Y).GE.PI) GO TO 2500
            GOX=LAMBDA+X
            GOY=PSI+Y
            CALL AZDIST(LAMBDA,PSI,GOX,GOY,AZGO,DIST)
            IF (DIST.LE.30.) GO TO 2600
2500        CONTINUE
            DIST=SQRT(X*X+Y*Y)
            X=X/DIST
            Y=Y/DIST
2600        CONTINUE
C REFINE INDICATED MOVE BY A GOLDEN SECTION SEARCH
            CALL SEARCH(LAMBDA,PSI,X,Y,DEGF)
            IF (KILL.EQ.2) GO TO 2700
            CALL SHIFT(SAVEL,SAVEP,LAMBDA,PSI,2,DEGF,DIST)
            GO TO 2800
2700        CALL AZDIST(SAVEL,SAVEP,LAMBDA,PSI,AZGO,DIST)
            SAVEL=LAMBDA
            SAVEP=PSI
C CHECK FOR MOVE LESS THAN MINIMUM STEP
2800        IF (DIST.LE.CUT) GO TO 3300
C SEARCHING STOPS AFTER 30 ITERATIONS UNLESS SEARCH PROGRESS
C IS REQUESTED
            IF (KILL.EQ.2) GO TO 2900
            IF (M.EQ.30) GO TO 3300
2900        CONTINUE
C IF THE SOLUTION HAS NOT BEEN FOUND, APPLY THE GOLDEN
C SECTION SEARCH AFTER EVERY TENTH ITERATION.
            IF (MOD(M,10).NE.0) GO TO 1600
            X=PIHALF
            Y=0.
            CALL SEARCH(LAMBDA,PSI,X,Y,DEGF)
            IF (KILL.EQ.2) GO TO 3000
            CALL SHIFT(SAVEL,SAVEP,LAMBDA,PSI,1,DEGF,DIST)
            GO TO 3100
3000        SAVEL=LAMBDA
            SAVEP=PSI
3100        X=0.
            Y=PIHALF
            CALL SEARCH(LAMBDA,PSI,X,Y,DEGF)
            IF (KILL.EQ.2) GO TO 3200
            CALL SHIFT(SAVEL,SAVEP,LAMBDA,PSI,1,DEGF,DIST)
            GO TO 1600
3200        SAVEL=LAMBDA
            SAVEP=PSI
            GO TO 1600
3300        DEGLAM=LAMBDA*RADDEG
            IF (DEGLAM.GT.180.) GO TO 3400
            X=SYMBOL(3)
            GO TO 3500
3400        DEGLAM=360.-DEGLAM
            X=SYMBOL(4)
3500        NDEGX=DEGLAM
            FDEG=NDEGX
            NMINX=(DEGLAM-FDEG)*60.+.5
            DEGPHI=ATAN(FNCECC*TAN(PSI))*RADDEG
            IF (DEGPHI.LT.0.) GO TO 3600
            Y=SYMBOL(1)
            GO TO 3700
```

```
3600    Y=SYMBOL(2)
        DEGPHI=-DEGPHI
3700    NDEGY=DEGPHI
        FDEG=NDEGY
        NMINY=(DEGPHI-FDEG)*60.+.5
        WRITE (6,2) NDEGX,NMINX,X,NDEGY,NMINY,Y
2       FORMAT ('0',30X,I3,'-',I2,A1,',',I3,'-',I2,A1,' IS THE
       1' LEAST SQUARES SOLUTION.')
        WRITE (6,3) DEGF
3       FORMAT (31X,' OBJECTIVE FUNCTION =',F8.2,' DEGREES',
       1' SQUARED.')
        WRITE (6,4) NUMBER
4       FORMAT (30X,I3,' DEGREES OF FREEDOM')
        WRITE (6,5)
5       FORMAT ('0',45X,'SOLUTION SIGNAL          SITE',/,30X,
       1' ID INTERCEPT   AZIMUTH   AZIMUTH        RANGE PLOT',
       2' THETA VALS',/,30X,' NR SITE NAME    BETA  -   THETA ',
       3'= OMEGA   NM    NORM  NM  AZ')
        SUMARC=0.
        DO 4000 K = 1,NUMBER
        ID=SITE(7,K)+.5
        DTHETA=THETA(K)*RADDEG
        CALL AZDIST(LAMBDA,PSI,SITE(1,K),SITE(4,K),SITEAZ,
       1DIST)
        NMSITE=DIST+.5
        ARCC=(DIST/3439.92)
        ANGLEB=ABS(DOMEGA(K))*DEGRAD
        ARCB=ARSIN(SIN(ANGLEB)*SIN(ARCC))
        ANGLEA=ARCOS(TAN(ARCB)*COTAN(ARCC))
        STAT=ARCC*RADDEG
        IF (STAT.GT.90.) STAT=180.-STAT
        IF (DOMEGA(K).GT.0.) GO TO 3800
        AZTHET=SITEAZ-ANGLEA*RADDEG
        IF (AZTHET.LT.0.) AZTHET=AZTHET+360.
        STAAZ(K)=AZTHET+90.
        IF (STAAZ(K).GT.360.) STAAZ(K)=STAAZ(K)-360.
        GO TO 3900
3800    AZTHET=SITEAZ+ANGLEA*RADDEG
        IF (AZTHET.GT.360.) AZTHET=AZTHET-360.
        STAAZ(K)=AZTHET-90.
        IF (STAAZ(K).LT.0.) STAAZ(K)=STAAZ(K)+360.
3900    NMTHET=ARCB*3439.92
        WRITE (6,6) ID,SITE(8,K),SITE(9,K),SITE(10,K),BETA(K),
       1DTHETA,DOMEGA(K),NMSITE,AZTHET,NMTHET,STAAZ(K)
6       FORMAT (30X,I3,1X,3A4,F8.3,F8.3,F7.3,I6,F6.1,I4,F6.1)
4000    SUMARC=SUMARC+STAT
        DNUM=NUMBER
        AVGARC=SUMARC/DNUM
        WRITE (6,7) AVGARC
7       FORMAT ('0',30X,'MEAN ARC STATISTIC =',F5.1,' DEGREES.
        CCUNT=0.
        SUMANG=0.
        NEND=NUMBER-1
        DO 4100 I = 1,NEND
        JBEGIN=I+1
        DO 4100 J = JBEGIN,NUMBER
        ACUTE=ABS(STAAZ(I)-STAAZ(J))
        IF (ACUTE.GT.180.) ACUTE=ACUTE-180.
        IF (ACUTE.GT.90.) ACUTE=180.-ACUTE
        SUMANG=SUMANG+ACUTE
4100    COUNT=COUNT+1.
        AVGANG=SUMANG/COUNT
        WRITE (6,8) AVGANG
8       FORMAT (31X,'MEAN ACUTE ANGLE OF INTERSECTION =',F5.1,
       1' DEGREES.')
        CALL PLOT (LAMBDA,PSI,DEGF,NUMBER)
        GO TO 0900
4200    CONTINUE
        STOP
        END
```

```
          SUBROUTINE SEARCH(L,P,X,Y,SAVEF)
C GOLDEN SECTION SEARCH
          REAL LAMBDA(2),L
          DIMENSION DEL(2),FDEL(2),PSI(2)
          COMMON/SITES/SITE(10,19),NUMBER
          COMMON/SIGNAL/THETA(19)
          DATA TWOPI/6.283185/,PIHALF/1.570796/,PI/3.141593/,
         1RADDEG/57.29578/
          SAVEL=L
          SAVEP=P
          IFLAG=0
          BEGIN=-1.
          END=1.
          J=1
1000      DEL(J)=0.618*BEGIN+0.382*END
          GO TO 1200
1100      IFLAG=2
          DEL(J)=0.382*BEGIN+0.618*END
1200      FDEL(J)=0.
          LAMBDA(J)=L+X*DEL(J)
          PSI(J)=P+Y*DEL(J)
C FIND CORRESPONDING TEST LONGITUDE IN THE INTERVAL
C (0,TWOPI).
          IF (LAMBDA(J).GT.TWOPI) LAMBDA(J)=LAMBDA(J)-TWOPI
          IF (LAMBDA(J).LT.0.) LAMBDA(J)=TWOPI+LAMBDA(J)
C FIND CORRESPONDING TEST LATITUDE IN THE INTERVAL
C (-PIHALF,PIHALF).
          IF (PSI(J).GT.PIHALF) PSI(J)=PI-PSI(J)
          IF (PSI(J).LT.-PIHALF) PSI(J)=-PI-PSI(J)
          COSLAM=COS(LAMBDA(J))
          SINLAM=SIN(LAMBDA(J))
          COSPSI=COS(PSI(J))
          SINPSI=SIN(PSI(J))
          VARLAM=LAMBDA(J)
          DO 1700 K = 1,NUMBER
          CALL AZCOMP(COSLAM,SINLAM,COSPSI,SINPSI,K,VARLAM,
         1A,B,C)
          TEST=A*B+C-THETA(K)
          IF (ABS(TEST)-PI) 1600,1600,1300
1300      IF (TEST) 1400,1600,1500
1400      C=C+TWOPI
          GO TO 1600
1500      C=C-TWOPI
1600      OMEGA=A*B+C-THETA(K)
1700      FDEL(J)=FDEL(J)+OMEGA**2
          IF (IFLAG.GT.1) GO TO 1800
          J=2
          GO TO 1100
1800      CONTINUE
C RETAIN VALUES CORRESPONDING TO CURRENT MINIMUM, ADJUST
C INTERVAL AND TEST NEXT DELTA SYMMETRIC WITH CURRENT DELTA.
          IF (FDEL(1)-FDEL(2)) 1900,1900,2000
1900      END=DEL(2)
          PSI(2)=PSI(1)
          LAMBDA(2)=LAMBDA(1)
          FDEL(2)=FDEL(1)
          DEL(2)=DEL(1)
          J=1
          GO TO 2100
2000      BEGIN=DEL(1)
          PSI(1)=PSI(2)
          LAMBDA(1)=LAMBDA(2)
          FDEL(1)=FDEL(2)
          DEL(1)=DEL(2)
          J=2
C TEST SIZE OF THE INTERVAL
2100      IF ((END-BEGIN).LE.0.01) GO TO 2200
          GO TO (1000,1100), J
```

```
2200      MIN=1
          IF (J.EQ.1) MIN=2
          L=LAMBDA(MIN)
          P=PSI(MIN)
          DELTA=DEL(MIN)
          DEGF=FDEL(MIN)*RADDEG**2
          IF (DEGF.LE.SAVEF) GO TO 2300
          L=SAVEL
          P=SAVEP
          RETURN
2300      SAVEF=DEGF
          RETURN
          END


          SUBROUTINE AZDIST(RLAM,RPSI,TLAM,TPSI,AZ,DIST)
C AZDIST COMPUTES AZIMUTH AND DISTANCE OF A TARGET WITH
C RESPECT TO A REFERENCE POINT
          DOUBLE PRECISION COSRP,SINRP,COSTP,SINTP,UC,RNUM,UG,
     1DEN,COSB,REFLAM,REFPSI,TARLAM,TARPSI,ARC
          DATA TWOPI/6.283185/,RADDEG/57.29578/,PI/3.141593/
          REFLAM=RLAM
          REFPSI=RPSI
          TARLAM=TLAM
          TARPSI=TPSI
          COSRP=DCOS(REFPSI)
          SINRP=DSIN(REFPSI)
          COSTP=DCOS(TARPSI)
          SINTP=DSIN(TARPSI)
          UC=DCOS(TARLAM)*DCOS(REFLAM)+DSIN(TARLAM)*DSIN(REFLAM)
          RNUM=SINTP*COSRP-COSTP*SINRP*UC
          UG=SINTP*SINRP+COSTP*COSRP*UC
          IF (UG.GE.1.0D0) UG=1.0D0
          IF (UG.LE.-1.0D0) UG=-1.0D0
          ARC=DARCOS(UG)
          DEN=DSIN(ARC)
          IF (DABS(ARC).LT.0.1D-4) GO TO 1600
          IF (DABS(RNUM).GT.0.0D-10) GO TO 1000
          COSB=0.0D0
          GO TO 1100
1000      COSB=RNUM/DEN
1100      CONTINUE
          COSB=RNUM/DEN
          IF (COSB.GE.1.0D0) COSB=1.0D0
          IF (COSB.LE.-1.0D0) COSB=-1.0D0
          BETA=DARCOS(COSB)
          TEST=REFLAM-TARLAM
          IF (TEST) 1200,1500,1300
1200      IF (TEST+PI) 1400,1500,1500
1300      IF (TEST-PI) 1400,1500,1500
1400      BETA=TWOPI-BETA
1500      AZ=BETA*RADDEG
          DIST=ARC*3439.92D0
          GO TO 1700
1600      AZ=0.
          DIST=0.
1700      CONTINUE
          RETURN
          END


          SUBROUTINE AZCOMP(COSLAM,SINLAM,COSPSI,SINPSI,K,
C AZCOMP COMPUTES POINT AZIMUTHS WITH RESPECT TO SITES
     1LAMBDA,A,B,C)
          REAL N,LAMBDA
          COMMON/SITES/SITE(10,19),NUMBER
          DATA PI/3.141593/,TWOPI/6.283185/,SCREEN/.9999999/
          A=1.
          C=0.
          UC=COSLAM*SITE(3,K)+SINLAM*SITE(2,K)
          N=SINPSI*SITE(6,K)-COSPSI*SITE(5,K)*UC
          UG=SINPSI*SITE(5,K)+COSPSI*SITE(6,K)*UC
```

```
      IF (UG.GE.1.) UG=SCREEN
      IF (UG.LE.-1.) UG=-SCREEN
      D=SIN(ARCOS(UG))
      COSB=N/D
      IF (COSB.GE.1.) COSB=SCREEN
      IF (COSB.LE.-1.) COSB=-SCREEN
      B=ARCOS(COSB)
      TEST=SITE(1,K)-LAMBDA
      IF (TEST) 1000,1300,1100
1000  IF (TEST+PI) 1200,1300,1300
1100  IF (TEST-PI) 1200,1300,1300
1200  A=-1
      C=TWOPI
1300  RETURN
      END


      SUBROUTINE SHIFT(FROML,FROMP,TOL,TOP,NRTYPE,DEGF,DIST)
C THIS SUBROUTINE COMPUTES AND WRITES SEARCH PROGRESS
      DIMENSION TYPES(2)
      DATA RADDEG/57.29578/, FNCECC/1.006768/
      DATA TYPES/'GOLD','GRAD'/
      CALL AZDIST(FROML,FROMP,TOL,TOP,AZGO,DIST)
      DEGLAM=TOL*RADDEG
      DEGPHI=ATAN(FNCECC*TAN(TOP))*RADDEG
      IF (NRTYPE.EQ.2) GO TO 1000
      TYPE=TYPES(1)
      GO TO 1100
1000  TYPE=TYPES(2)
1100  WRITE (6,1) TYPE,DIST,AZGO,DEGLAM,DEGPHI,DEGF
1     FORMAT (31X,A4,F7.1,' NM ON AZ',F6.1,' TO',F8.3,'E',
     1F8.3,'. F=',F10.3)
      FROML=TOL
      FROMP=TOP
      RETURN
      END


      SUBROUTINE PLOT(LAMBDA,PSI,DEGF,NUMBER)
C PLOT COMPUTES AND WRITES THE CONFIDENCE REGION
      REAL LAMBDA,L
      DOUBLE PRECISION VARPSI,PIHALF,PI,ARC,COSCOL,COLAT,
     1COSANG
      COMMON/SIGNAL/THETA(19)
      DIMENSION OUT(52),SYMBOL(3)
      DIMENSION CHI900(19)
      DIMENSION JSCALE(11)
      DATA SYMBOL/'*',' ','S'/
      DATA PIHALF/1.5707963260D0/,PI/3.141592653D0/
      DATA DEGRAD/1.745329E-2/,TWOPI/6.283185/,
     1RADDEG/57.29578/
      DATA CHI900/2.71,4.61,6.25,7.78,9.24,10.6,12.0,13.4,
     114.7,16.,17.3,18.5,19.8,21.1,22.3,23.5,24.8,26.,27.2/
      BOUND=CHI900(NUMBER)
      PROB=.900
      NSIZE=400
0900  SIZE=NSIZE/2
      TOP=PSI+1.05*SIZE*2.9070443E-4
      KCUNT=0
      MARKV=0
      DO 2700 I = 1,41
      ADD=0.
      IF (MARV.NE.2) GO TO 1100
      DO 1000 J = 1,51
      OUT(J)=SYMBOL(1)
1000  CONTINUE
      GO TO 2500
1100  TAKE=I
      DIRECT=1.
      VARPSI=TOP-TAKE*0.05*SIZE*2.9070443E-4
      IF (VARPSI.LT.PIHALF) GO TO 1200
      VARPSI=PI-VARPSI
```

```
               DIRECT=-1.
               ADD=PI
               GO TO 1300
      1200     IF (VARPSI.GT.-PIHALF) GO TO 1300
               VARPSI=-PI-VARPSI
               DIRECT=-1.
               ADD=PI
      1300     PARC=1.04*SIZE*2.9070443E-4
               MARKH=0
               DO 2500 J = 1,51
               IF (MARKH.EQ.2) GO TO 2100
               TAKE=J
               ARC=PARC-TAKE*0.04*SIZE*2.9070443E-4
               COSCOL=DCOS(ARC)*DSIN(VARPSI)
               IF (COSCOL.GT.1.D0) COSCOL=1.D0
               IF (COSCOL.LT.-1.D0) COSCOL=-1.D0
               COLAT=DARCOS(COSCOL)
               P=PIHALF-COLAT
               COSANG=DCOTAN(VARPSI)*DCOTAN(COLAT)
               IF (COSANG.GT.1.D0) COSANG=1.D0
               IF (COSANG.LT.-1.D0) COSANG=-1.D0
               ANGLE=DARCOS(COSANG)
               IF (J.LE.26) GO TO 1400
               L=LAMBDA+DIRECT*ANGLE+ADD
               GO TO 1500
      1400     L=LAMBDA--DIRECT*ANGLE+ADD
      1500     CONTINUE
               IF (L.GT.TWOPI) L=L-TWOPI
               IF (L.LT.0.) L=TWOPI+L
               COSLAM=COS(L)
               SINLAM=SIN(L)
               COSPSI=COS(P)
               SINPSI=SIN(P)
               DEGF=0.
               DO 2000 K = 1,NUMBER
               CALL AZCOMP(COSLAM,SINLAM,COSPSI,SINPSI,K,L,A,B,C)
               TEST=A*B+C-THETA(K)
               IF (ABS(TEST)-PI) 1900,1900,1600
      1600     IF (TEST) 1700,1900,1800
      1700     C=C+TWOPI
               GO TO 1900
      1800     C=C-TWOPI
      1900     OMEGA=A*B+C-THETA(K)
      2000     DEGF=DEGF+(OMEGA*RADDEG)**2
      2100     OUT(J)=SYMBOL(1)
               MARKER=MARKH+1
               GO TO (2300,2200,2500), MARKER
      2200     IF (DEGF.GT.BOUND) MARKH=2
      2300     IF (DEGF.GT.BOUND) GO TO 2400
               OUT(J)=SYMBOL(2)
               KOUNT=KOUNT+1
               MARKH=1
               MARKV=1
               IF (I.GT.1) GO TO 2350
               NSIZE=NSIZE+200
               GO TO 0900
      2350     IF (J.GT.1) GO TO 2400
               NSIZE=NSIZE+NSIZE
               WRITE (6,7)
      7        FORMAT ('1')
               GO TO 0900
      2400     IF (I.NE.21) GO TO 2500
               IF (J.EQ.26) OUT(J)=SYMBOL(3)
      2500     CONTINUE
               IF (MARKV.NE.1) GO TO 2600
               IF (MARKH.EQ.0) MARKV=2
      2600     CONTINUE
               IF (I.NE.1) GO TO 2650
               WRITE (6,1) PROB,NSIZE,NSIZE
      1        FORMAT ('0',30X,F6.3,' CONFIDENCE REGION PLOT ON',I5,
              1' NM BY',I5,' NM AREA')
               WRITE (6,3)
```

95

```
3         FORMAT (37X,17('----'),'--')
2650      CONTINUE
          VERT=21-I
          NM=ABS(0.05*VERT*SIZE)+.5
          IF (I.GT.21) NM=-NM
          WRITE (6,4) NM,(CUT(J),J=1,51)
4         FORMAT (' ',30X,I5,' I',51A1,'I')
2700      CONTINUE
          WRITE (6,3)
          DO 2800 J = 1,11
          ADD=J
          JSCALE(J)=ABS((0.2*ADD-1.2)*SIZE)+.5
2800      IF (J.LT.6) JSCALE(J)=-JSCALE(J)
          WRITE (6,5) (JSCALE(J),J=1,11)
5         FORMAT (34X,11I5)
          IJAREA=0.002*SIZE**2+.5
          NMAREA=KCUNT*IJAREA
          WRITE (6,6) NMAREA
6         FORMAT (30X,'       CONFIDENCE REGION AREA =',I7,
         1' NAUTICAL MILES SQUARED.')
          RETURN
          END
```

```
GOLD 4398.4 NM ON AZ 270.0 TO 286.740E    0.0  . F=  20254.277
GOLD 4675.4 NM ON AZ 180.0 TO 286.740E -77.953. F=  11288.250
GOLD 1021.9 NM ON AZ 134.1 TO  16.323E -77.953. F=   8562.371
GOLD 1898.3 NM ON AZ   0.0 TO  16.323E -46.449. F=   3712.686
GOLD 1108.5 NM ON AZ  99.8 TO  43.155E -46.449. F=    868.700
GOLD  412.8 NM ON AZ   0.0 TO  43.155E -39.571. F=    111.312
GRAD  271.3 NM ON AZ  94.0 TO  49.004E -39.741. F=     15.526
GRAD   84.6 NM ON AZ  53.8 TO  50.461E -38.898. F=      0.158
GRAD   10.2 NM ON AZ  76.8 TO  50.673E -38.859. F=      0.050
GRAD    0.1 NM ON AZ  52.7 TO  50.675E -38.858. F=      0.050
```

50-40E, 38-51S IS THE LEAST SQUARES SOLUTION.
OBJECTIVE FUNCTION =   0.05 DEGREES SQUARED.
3 DEGREES OF FREEDOM

```
                   SOLUTION SIGNAL              SITE
ID INTERCEPT       AZIMUTH  AZIMUTH             RANGE PLOT THETA VALS
NR SITE NAME       BETA  -  THETA  = OMEGA      NM    NORM  NM   AZ
 9 HONOLULU        228.098  228.241  -0.142     9001   27.1   4 117.1
19 WICHITA         102.627  102.797  -0.170     9301  187.3   4 277.3
10 LOS ANGELES     121.457  121.424   0.033    10199  335.1   0 245.1
```

MEAN ARC STATISTIC = 21.8 DEGREES.
MEAN ACUTE ANGLE OF INTERSECTION = 34.7 DEGREES.

0.900 CONFIDENCE REGION PLOT ON 400 NM BY 400 NM AREA
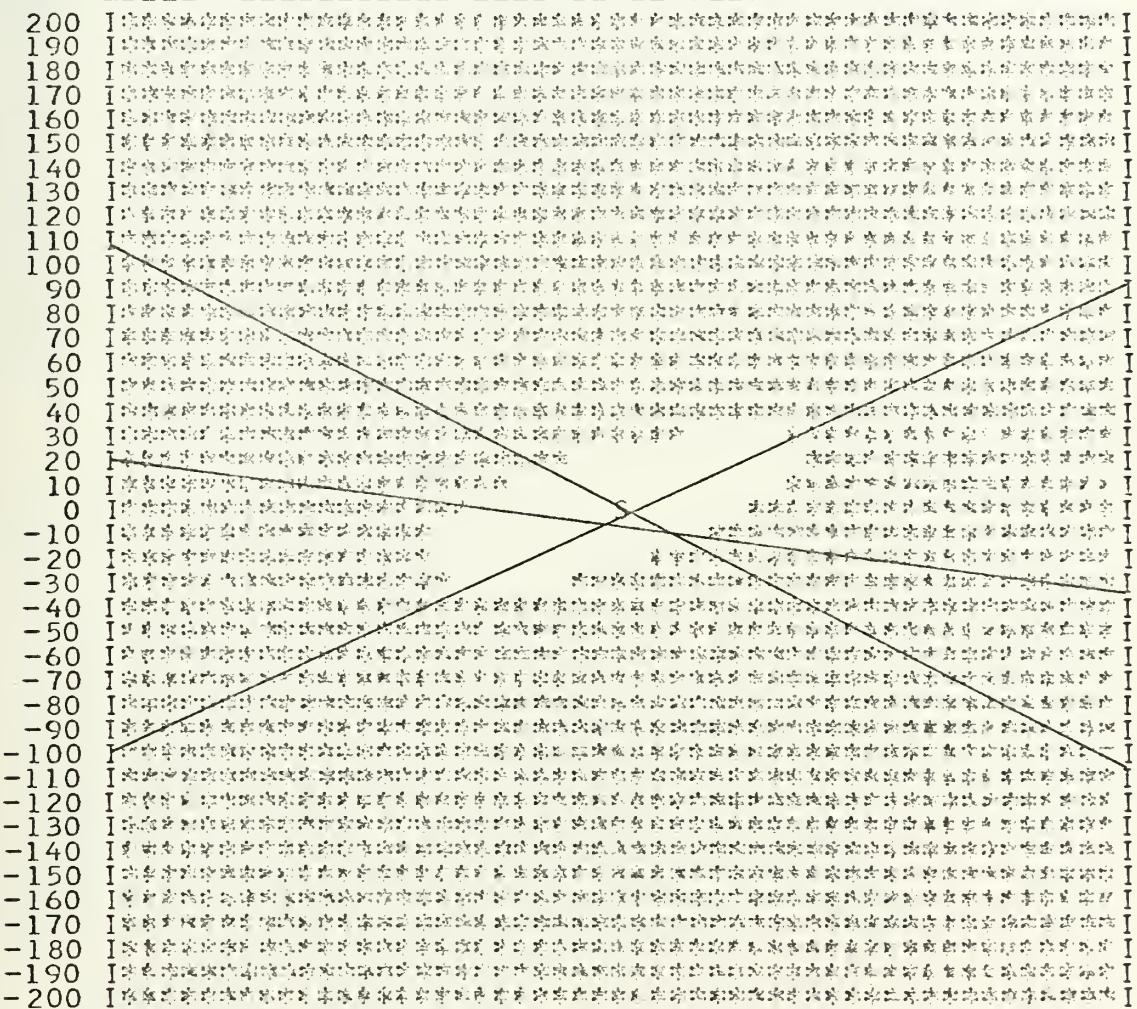
CONFIDENCE REGION AREA =   6080 NAUTICAL MILES SQUARED.

97

```
GOLD 6104.5 NM ON AZ 270.0 TO 258.323E    0.0 .  F=   86.016
GOLD  276.9 NM ON AZ 180.0 TO 258.323E   -4.643.  F=   79.381
GRAD 2293.2 NM ON AZ 167.1 TO 268.963E  -41.796.  F=   10.165
GRAD 1199.7 NM ON AZ 160.2 TO 282.300E  -59.978.  F=    0.043
GRAD   77.3 NM ON AZ 151.7 TO 283.557E  -61.102.  F=    0.013
GRAD    0.9 NM ON AZ  97.3 TO 283.589E  -61.104.  F=    0.013
GRAD    0.0 NM ON AZ   0.0 TO 283.590E  -61.104.  F=    0.013
```

76-25W, 61- 6S IS THE LEAST SQUARES SOLUTION.
OBJECTIVE FUNCTION =   0.01 DEGREES SQUARED.
3 DEGREES OF FREEDOM

```
                    SOLUTION SIGNAL        SITE
ID INTERCEPT        AZIMUTH  AZIMUTH       RANGE PLOT THETA VALS
NR SITE NAME        BETA  -  THETA = OMEGA NM    NORM  NM   AZ
 7 EL PASO          165.841  165.922 -0.081 5747 244.6   4 334.6
17 RENO             159.655  159.655  0.000 6383  56.4   0 326.4
 8 HELENA           162.349  162.270  0.080 6673  64.5   4 334.5
```

MEAN ARC STATISTIC = 75.6 DEGREES.
MEAN ACUTE ANGLE OF INTERSECTION =   5.5 DEGREES.

0.900 CONFIDENCE REGION PLOT ON 2400 NM BY 2400 NM AREA

CONFIDENCE REGION AREA = 311040 NAUTICAL MILES SQUARED.

98

```
GOLD  7810.8 NM ON AZ 270.0 TO 229.901E   0.0  . F=    663.993
GOLD   995.3 NM ON AZ 180.0 TO 229.901E -16.684. F=     13.884
GOLD    97.0 NM ON AZ  90.2 TO 231.588E -16.684. F=      3.408
GOLD     3.8 NM ON AZ   0.0 TO 231.588E -16.620. F=      3.381
GRAD    10.1 NM ON AZ  67.7 TO 231.750E -16.556. F=      3.289
GRAD     0.0 NM ON AZ   0.0 TO 231.750E -16.556. F=      3.289
```

128-15W, 16-33S IS THE LEAST SQUARES SOLUTION.
 OBJECTIVE FUNCTION =   3.29 DEGREES SQUARED.
 4 DEGREES OF FREEDOM

```
                   SOLUTION SIGNAL           SITE
ID INTERCEPT       AZIMUTH  AZIMUTH          RANGE PLOT THETA VALS
NR SITE NAME       BETA  -  THETA = OMEGA    NM    NORM  NM   AZ
14 NASHVILLE       224.264  224.377 -0.113   3929  306.1  6   36.1
 2 ATTU            124.892  126.340 -1.448   5135  238.9  86  328.9
 9 HONOLULU        140.026  138.983  1.043   2854   50.6  46  320.6
16 NORFOLK         232.077  231.774  0.303   4406  130.0  17   40.0
```

MEAN ARC STATISTIC = 68.0 DEGREES.
MEAN ACUTE ANGLE OF INTERSECTION = 50.9 DEGREES.

 0.900 CONFIDENCE REGION PLOT ON 400 NM BY 400 NM AREA

CONFIDENCE REGION AREA = 20880 NAUTICAL MILES SQUARED.

99
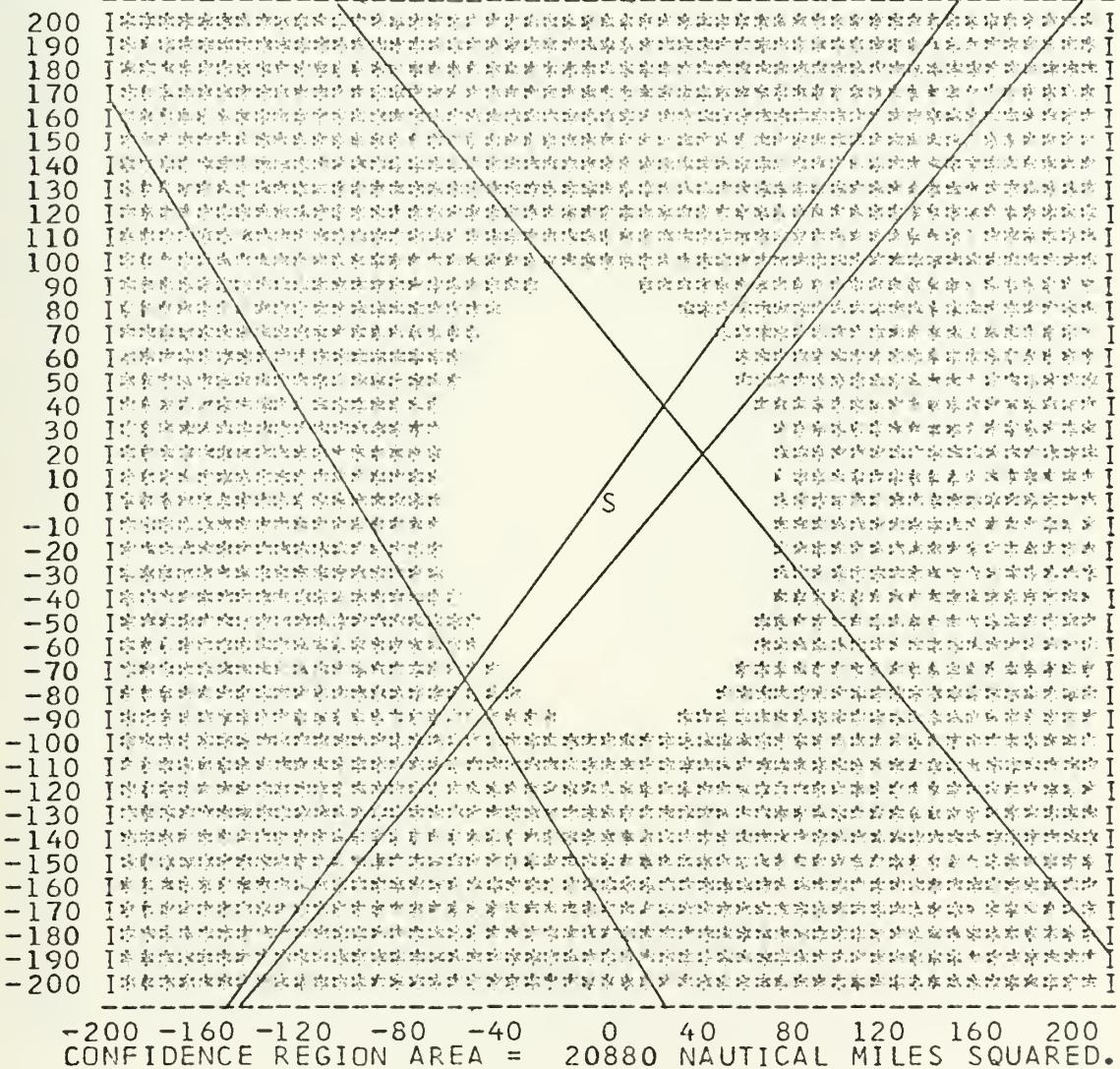
```
GOLD 4399.1 NM ON AZ  90.0 TO  73.272E   0.0  . F=   767.351
GOLD 1765.6 NM ON AZ   0.0 TO  73.272E  29.574. F=    26.527
GOLD  123.9 NM ON AZ  89.4 TO  75.642E  29.574. F=     4.538
GOLD   71.1 NM ON AZ   0.0 TO  75.642E  30.763. F=     3.487
GRAD   14.2 NM ON AZ  55.7 TO  75.869E  30.897. F=     3.303
GRAD    0.2 NM ON AZ  40.6 TO  75.871E  30.899. F=     3.303
GRAD    0.0 NM ON AZ   0.0 TO  75.871E  30.899. F=     3.303
```

75-52E, 30-54N IS THE LEAST SQUARES SOLUTION.
OBJECTIVE FUNCTION =   3.30 DEGREES SQUARED.
5 DEGREES OF FREEDOM

ID NR	INTERCEPT SITE NAME	SOLUTION AZIMUTH BETA	SIGNAL AZIMUTH – THETA	= OMEGA	SITE RANGE NM	PLOT NORM	THETA VALS NM	AZ
17	RENO	345.832	345.356	0.476	6511	102.9	27	12.9
5	DENVER	359.185	358.897	0.288	6589	90.8	16	0.8
12	MIDWAY	304.587	304.956	-0.369	5329	327.7	22	57.7
19	WICHITA	6.275	7.726	-1.451	6693	263.7	81	353.7
7	EL PASO	357.715	356.849	0.866	7064	92.7	46	2.7

MEAN ARC STATISTIC = 72.3 DEGREES.
MEAN ACUTE ANGLE OF INTERSECTION = 28.0 DEGREES.

0.900 CONFIDENCE REGION PLOT ON 400 NM BY 400 NM AREA
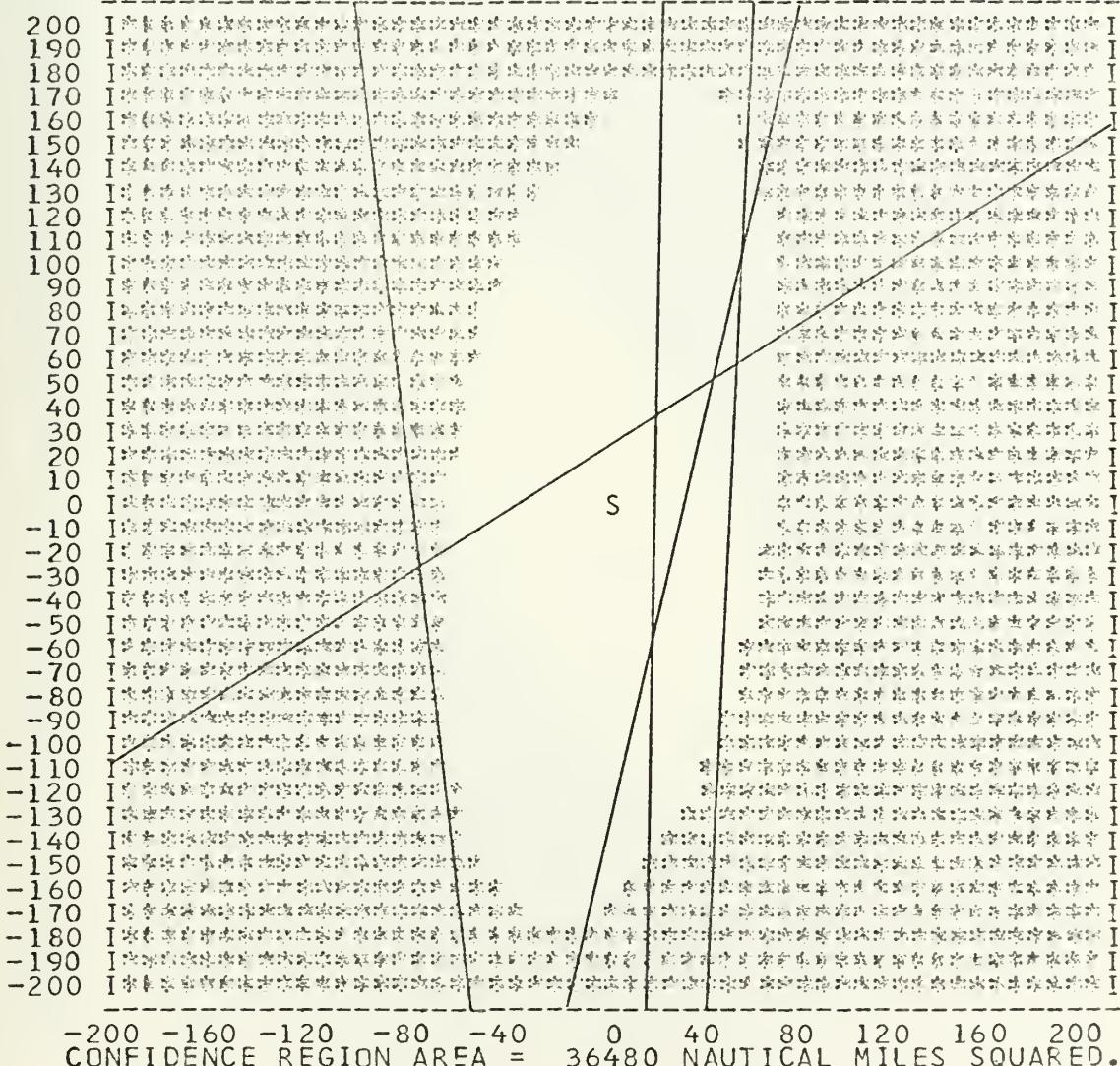

```
    -200 -160 -120  -80  -40   0   40   80  120  160  200
```
CONFIDENCE REGION AREA = 36480 NAUTICAL MILES SQUARED.

```
GOLD 2476.5 NM ON AZ  90.0 TO  41.249E   0.0   . F=   258.677
GOLD  561.3 NM ON AZ   0.0 TO  41.249E   9.411. F=    94.282
GOLD  207.1 NM ON AZ 270.3 TO  37.754E   9.411. F=    42.317
GOLD  213.3 NM ON AZ   0.0 TO  37.754E  12.985. F=    20.378
GRAD  277.8 NM ON AZ 318.0 TO  34.526E  16.421. F=     0.264
GRAD    4.4 NM ON AZ 325.8 TO  34.483E  16.482. F=     0.259
GRAD    0.1 NM ON AZ 325.7 TO  34.482E  16.484. F=     0.259
GRAD    0.0 NM ON AZ   0.0 TO  34.482E  16.484. F=     0.259
```

34-29E, 16-29N IS THE LEAST SQUARES SOLUTION.
OBJECTIVE FUNCTION =   0.26 DEGREES SQUARED.
5 DEGREES OF FREEDOM

ID NR	INTERCEPT SITE NAME	SOLUTION AZIMUTH BETA –	SIGNAL AZIMUTH THETA =	OMEGA	SITE RANGE NM	PLOT NORM NM	THETA VALS NM AZ	
8	HELENA	34.383	33.967	0.417	6624	66.2	23	336.2
11	MIAMI	63.878	64.000	-0.122	6235	212.4	7	302.4
14	NASHVILLE	57.577	57.539	0.038	6229	44.6	2	314.6
17	RENO	28.527	28.765	-0.238	7165	247.2	12	337.2
1	ANCHORAGE	355.710	355.825	-0.114	6153	272.1	6	2.1

MEAN ARC STATISTIC = 72.1 DEGREES.
MEAN ACUTE ANGLE OF INTERSECTION = 28.4 DEGREES.

0.900 CONFIDENCE REGION PLOT ON 600 NM BY 600 NM AREA


```
           -300 -240 -180 -120  -60    0   60  120  180  240  300
```
CONFIDENCE REGION AREA =   57600 NAUTICAL MILES SQUARED.

101

```
GOLD 1690.8 NM ON AZ 270.0 TO 331.837E    0.0  . F=    102.897
GOLD  141.5 NM ON AZ 180.0 TO 331.837E   -2.373. F=     83.012
GRAD  629.1 NM ON AZ 135.7 TO 339.241E   -9.884. F=      3.863
GRAD    2.2 NM ON AZ  51.3 TO 339.270E   -9.861. F=      3.846
GRAD    0.1 NM ON AZ  48.4 TO 339.271E   -9.860. F=      3.845
```

20-44W. 9-52S IS THE LEAST SQUARES SOLUTION.
OBJECTIVE FUNCTION =   3.85 DEGREES SQUARED.
6 DEGREES OF FREEDOM

		SOLUTION	SIGNAL		SITE			
ID	INTERCEPT	AZIMUTH	AZIMUTH		RANGE	PLOT	THETA	VALS
NR	SITE NAME	BETA -	THETA =	OMEGA	NM	NORM	NM	AZ
3	BOSTON	125.857	125.554	0.303	4166	52.3	17	322.3
12	MIDWAY	54.831	54.455	0.376	9092	43.3	10	313.3
2	ATTU	19.885	19.173	0.712	8140	78.4	29	348.4
11	MIAMI	113.543	114.172	-0.629	4071	213.2	34	303.2
1	ANCHORAGE	58.837	60.428	-1.591	7009	244.4	85	334.4
10	LOS ANGELES	94.063	93.642	0.421	6103	32.9	24	302.9

MEAN ARC STATISTIC = 58.6 DEGREES.
MEAN ACUTE ANGLE OF INTERSECTION = 22.0 DEGREES.

0.900 CONFIDENCE REGION PLOT ON 400 NM BY 400 NM AREA


```
       -200 -160 -120  -80  -40   0   40   80  120  160  200
```
CONFIDENCE REGION AREA =   26720 NAUTICAL MILES SQUARED.

```
GOLD 7158.7 NM ON AZ   90.0 TO 119.236E    0.0  . F=    318.482
GOLD  251.0 NM ON AZ    0.0 TO 119.236E    4.209. F=    261.669
GRAD 1861.3 NM ON AZ   29.7 TO 136.486E   30.744. F=     34.133
GRAD  525.6 NM ON AZ   47.2 TO 144.451E   36.464. F=      8.503
GRAD  104.9 NM ON AZ   34.4 TO 145.701E   37.901. F=      8.042
GRAD    5.3 NM ON AZ  222.2 TO 145.627E   37.836. F=      8.041
GRAD    0.6 NM ON AZ  222.0 TO 145.618E   37.829. F=      8.041
GRAD    0.4 NM ON AZ  221.9 TO 145.612E   37.824. F=      8.041
GRAD    0.1 NM ON AZ  221.8 TO 145.611E   37.822. F=      8.041
GRAD    0.0 NM ON AZ    0.0 TO 145.611E   37.822. F=      8.041
```

145-37E. 37-49N IS THE LEAST SQUARES SOLUTION.
 OBJECTIVE FUNCTION =   8.04 DEGREES SQUARED.
 6 DEGREES OF FREEDOM

```
                   SOLUTION SIGNAL           SITE
ID INTERCEPT       AZIMUTH  AZIMUTH          RANGE PLOT THETA VALS
NR SITE NAME       BETA  -  THETA = OMEGA    NM    NORM  NM   AZ
16 NORFOLK         327.990  328.189  -0.199  5685  301.6  11  31.6
 4 CORPUS CHRIS    315.081  314.619   0.462  5524  142.2  27  52.2
11 MIAMI           324.266  322.103   2.164  6215  132.2 126  42.2
18 SEATTLE         298.750  300.372  -1.622  3873  319.2  87  49.2
 6 DETROIT         323.507  324.197  -0.690  5328  303.9  41  33.9
13 MINNEAPOLIS     316.823  316.840  -0.016  4923  307.8   0  37.8
```

MEAN ARC STATISTIC = 80.8 DEGREES.
MEAN ACUTE ANGLE OF INTERSECTION = 10.2 DEGREES.

 0.900 CONFIDENCE REGION PLOT ON 600 NM BY 600 NM AREA

CONFIDENCE REGION AREA =   37080 NAUTICAL MILES SQUARED.

103

```
GOLD 2341.5 NM ON AZ   90.0 TO   39.000E    0.0  .  F=  5868.273
GOLD  575.9 NM ON AZ  180.0 TO   39.000E   -9.656.  F=  5288.270
GOLD  486.3 NM ON AZ   90.7 TO   47.215E   -9.656.  F=  4666.781
GOLD  531.3 NM ON AZ  180.0 TO   47.215E  -18.558.  F=  3902.349
GOLD  406.6 NM ON AZ   91.1 TO   54.355E  -18.558.  F=  3082.319
GOLD  426.4 NM ON AZ  180.0 TO   54.355E  -25.695.  F=  2172.056
GRAD  577.5 NM ON AZ  138.9 TO   61.849E  -32.774.  F=   215.962
GRAD   95.2 NM ON AZ   36.1 TO   62.942E  -31.483.  F=     4.374
GRAD   10.9 NM ON AZ   99.8 TO   63.151E  -31.514.  F=     2.152
GRAD    0.1 NM ON AZ   25.4 TO   63.152E  -31.512.  F=     2.152
GRAD    0.0 NM ON AZ    0.0 TO   63.152E  -31.512.  F=     2.152
```

63- 9E, 31-31S IS THE LEAST SQUARES SOLUTION.
OBJECTIVE FUNCTION =   2.15 DEGREES SQUARED.
7 DEGREES OF FREEDOM

```
                 SOLUTION SIGNAL           SITE
ID INTERCEPT     AZIMUTH  AZIMUTH          RANGE  PLOT THETA VALS
NR SITE NAME     BETA  -  THETA = OMEGA    NM     NORM  NM    AZ
 5 DENVER         53.228   53.230  -0.002  10049  223.7   0  313.7
15 NEW ORLEANS   100.649  101.286  -0.637   9425  182.5  14  272.5
 6 DETROIT        79.209   78.237   0.972   9070   32.3  28  302.3
16 NORFOLK        90.386   89.567   0.820   8779   24.3  27  294.3
 7 EL PASO        91.177   91.369  -0.192  10276  184.1   1  274.1
17 RENO          342.343  342.395  -0.051  10306  285.9   0   15.9
 8 HELENA         15.592   15.892  -0.300   9875  257.2   4  347.2
```

MEAN ARC STATISTIC = 18.7 DEGREES.
MEAN ACUTE ANGLE OF INTERSECTION = 42.9 DEGREES.

0.900 CONFIDENCE REGION PLOT ON 400 NM BY 400 NM AREA
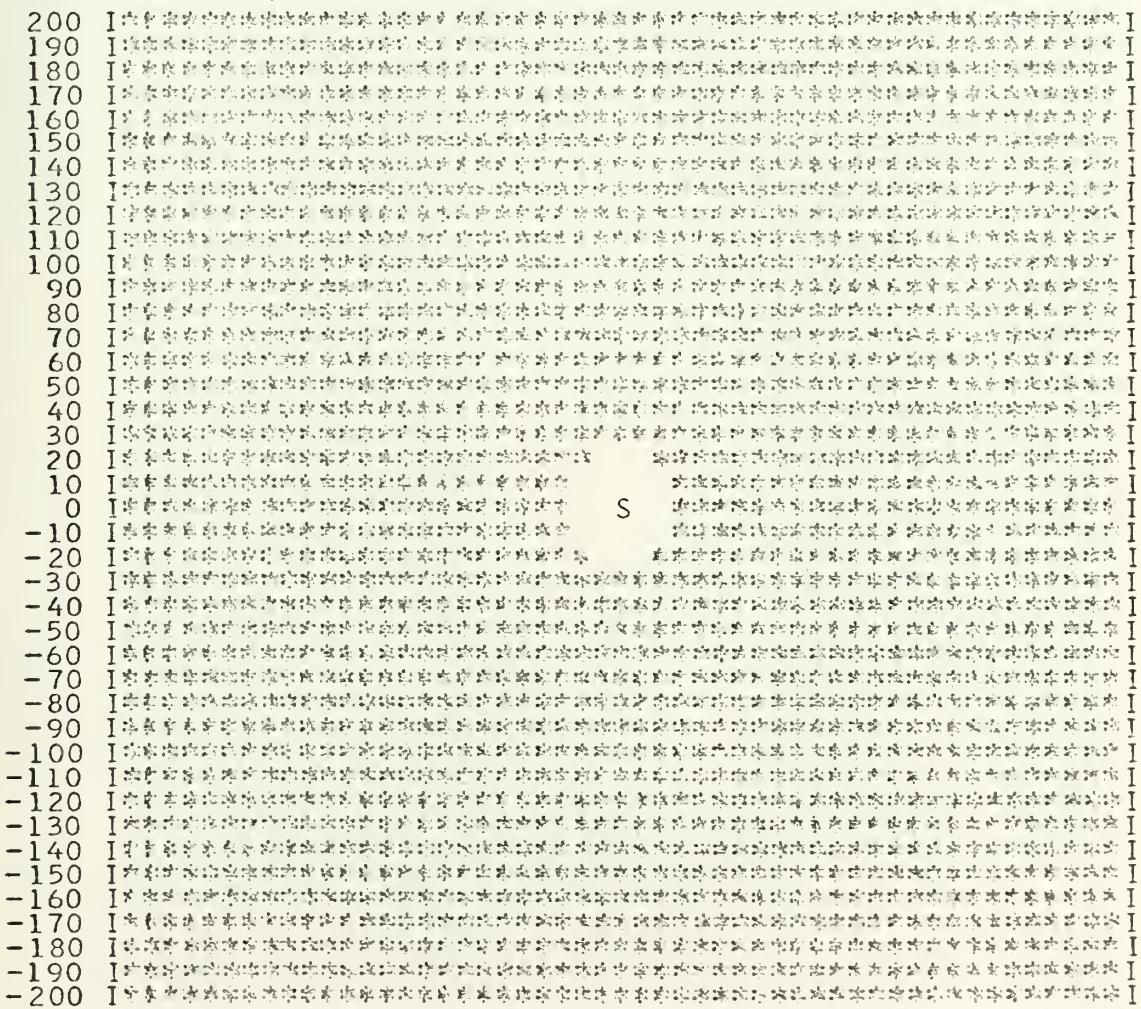
CONFIDENCE REGION AREA =   1680 NAUTICAL MILES SQUARED.

```
GOLD 5019.9 NM ON AZ 270.0 TO 276.387E   0.0  . F=    348.028
GOLD  819.4 NM ON AZ 180.0 TO 276.387E -13.737. F=     15.774
GOLD   73.1 NM ON AZ  90.1 TO 277.641E -13.737. F=      5.151
GOLD   71.1 NM ON AZ 180.0 TO 277.641E -14.929. F=      2.936
GRAD    1.4 NM ON AZ 267.9 TO 277.616E -14.930. F=      2.927
GRAD    0.1 NM ON AZ 270.0 TO 277.615E -14.930. F=      2.926
```

82-23W, 14-56S IS THE LEAST SQUARES SOLUTION.
OBJECTIVE FUNCTION =   2.93 DEGREES SQUARED.
8 DEGREES OF FREEDOM

ID NR	INTERCEPT SITE NAME	SOLUTION AZIMUTH BETA –	SIGNAL AZIMUTH THETA	= OMEGA	SITE RANGE NM	PLOT NORM	THETA NM	VALS AZ
9	HONOLULU	109.222	109.844	-0.622	4943	204.5	36	294.5
17	RENO	139.373	138.901	0.472	3868	58.4	25	328.4
6	DETROIT	179.229	179.163	0.066	3421	89.4	3	359.4
14	NASHVILLE	174.501	173.573	0.928	3060	84.8	43	354.8
3	BOSTON	192.934	193.473	-0.539	3479	280.2	27	10.2
11	MIAMI	183.252	184.030	-0.778	2432	273.6	30	3.6
19	WICHITA	162.091	161.478	0.613	3253	75.0	29	345.0
8	HELENA	148.667	149.088	-0.421	4010	248.4	23	338.4

MEAN ARC STATISTIC = 59.3 DEGREES.
MEAN ACUTE ANGLE OF INTERSECTION = 27.8 DEGREES.

0.900 CONFIDENCE REGION PLOT ON 400 NM BY 400 NM AREA


```
     -200 -160 -120  -80  -40   0   40   80  120  160  200
CONFIDENCE REGION AREA =   33040 NAUTICAL MILES SQUARED.
```

105

```
GOLD  9485.0 NM ON AZ   90.0 TO 157.984E    0.0  .  F=    215.253
GOLD    74.4 NM ON AZ    0.0 TO 157.984E    1.248.  F=    207.475
GRAD  1077.6 NM ON AZ   51.3 TO 172.232E   12.394.  F=      6.162
GRAD    13.2 NM ON AZ   15.4 TO 172.292E   12.607.  F=      5.864
GRAD     0.0 NM ON AZ    0.0 TO 172.292E   12.607.  F=      5.864
```

172-18E, 12-36N IS THE LEAST SQUARES SOLUTION.
 OBJECTIVE FUNCTION =   5.86 DEGREES SQUARED.
 9 DEGREES OF FREEDOM

```
                       SOLUTION SIGNAL          SITE
ID INTERCEPT           AZIMUTH  AZIMUTH         RANGE PLOT THETA VALS
NR SITE NAME           BETA  -  THETA = OMEGA   NM    NORM  NM   AZ
 9 HONOLULU            257.935  258.530  -0.594 1788  339.6  17  69.6
10 LOS ANGELES         269.320  268.506   0.814 3968  147.9  44  57.9
11 MIAMI               289.107  288.596   0.511 5995  150.9  30  60.9
12 MIDWAY              213.947  213.857   0.090 1098  120.2   1  30.2
13 MINNEAPOLIS         282.050  282.304  -0.254 5064  315.3  15  45.3
14 NASHVILLE           286.504  286.771  -0.267 5480  322.6  16  52.6
15 NEW ORLEANS         284.612  282.885   1.727 5418  149.3 103  59.3
16 NORFOLK             293.348  293.874  -0.526 5903  317.3  31  47.3
17 RENO                265.894  266.982  -1.088 3907  322.7  59  52.7
```

MEAN ARC STATISTIC = 67.1 DEGREES.
MEAN ACUTE ANGLE OF INTERSECTION = 13.0 DEGREES.

0.900 CONFIDENCE REGION PLOT ON 400 NM BY 400 NM AREA


```
      -200 -160 -120  -80  -40   0   40   80  120  160  200
       CONFIDENCE REGION AREA =   18080 NAUTICAL MILES SQUARED.
```

```
GOLD  202.5 NM ON AZ  90.0 TO    3.373E    0.0 . F= 10268.355
GOLD 1955.9 NM ON AZ   0.0 TO    3.373E   32.769. F=  5296.391
GOLD 1314.5 NM ON AZ 277.1 TO  337.319E   32.769. F=  3449.257
GOLD  585.4 NM ON AZ   0.0 TO  337.319E   42.536. F=  2502.434
GOLD 2030.4 NM ON AZ 286.1 TO  290.972E   42.536. F=   119.602
GOLD   56.1 NM ON AZ   0.0 TO  290.972E   43.471. F=    51.410
GRAD  107.2 NM ON AZ  69.9 TO  293.299E   44.062. F=    10.708
GRAD    4.2 NM ON AZ 216.4 TO  293.241E   44.006. F=    10.553
GRAD    0.1 NM ON AZ 215.9 TO  293.240E   44.005. F=    10.553
```

66-46W, 44- ON IS THE LEAST SQUARES SOLUTION.
OBJECTIVE FUNCTION =   10.55 DEGREES SQUARED.
9 DEGREES OF FREEDOM

		SOLUTION	SIGNAL			SITE			
ID	INTERCEPT	AZIMUTH	AZIMUTH			RANGE	PLOT	THETA	VALS
NR	SITE NAME	BETA	-	THETA	= OMEGA	NM	NORM	NM	AZ
6	DETROIT	76.495		77.395	-0.900	721	178.5	11	268.5
12	MIDWAY	42.761		41.147	1.614	5054	33.7	96	303.7
18	SEATTLE	74.220		72.903	1.317	2294	24.5	48	294.5
5	DENVER	68.794		67.963	0.832	1719	4.1	23	274.1
11	MIAMI	27.603		26.907	0.696	1274	304.7	15	214.7
17	RENO	65.683		66.781	-1.098	2357	193.2	41	283.2
4	CORPUS CHRIS	48.511		47.035	1.476	1765	335.6	43	245.6
10	LOS ANGELES	60.122		60.990	-0.868	2440	184.6	33	274.6
16	NORFOLK	50.167		50.470	-0.303	534	146.7	2	236.7

MEAN ARC STATISTIC = 33.6 DEGREES.
MEAN ACUTE ANGLE OF INTERSECTION = 33.9 DEGREES.

0.900 CONFIDENCE REGION PLOT ON 400 NM BY 400 NM AREA
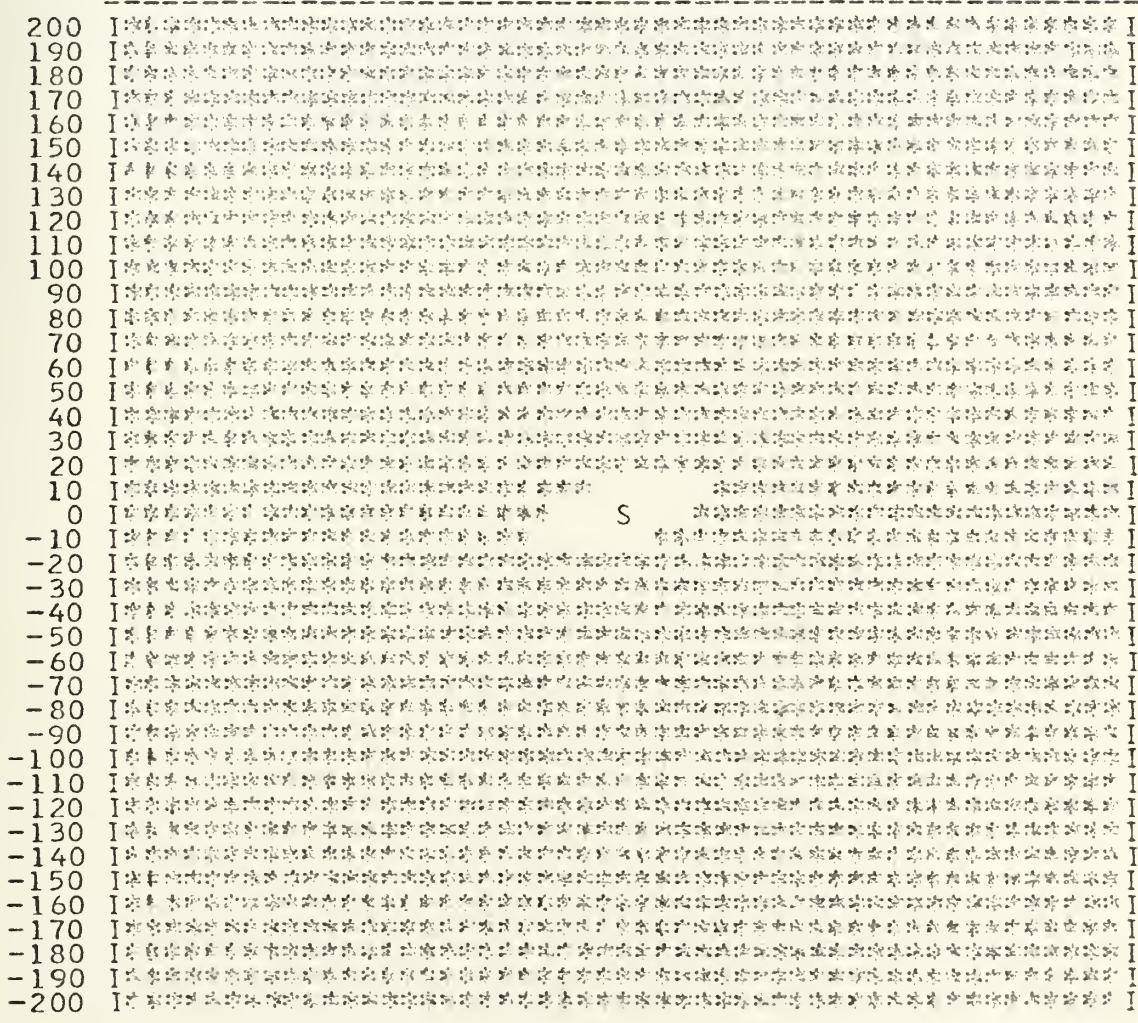
CONFIDENCE REGION AREA =   1520 NAUTICAL MILES SQUARED.

107

LIST OF REFERENCES

1. Wilde, D. J., Optimal Seeking Methods, Prentice Hall,
        Englewood Cliffs, N.J., 1969.

2. Hoel, P.G., Port, S. C., and Stone, C. J., Introduction
        to Probability Theory, Houghton Mifflin, Boston,
        1971.

3. Encyclopaedia Britannica, 1972.

4. Daniels, H. E., "The Theory of Position Finding,"
        Journal of the Royal Statistical Society, B, 13, 2,
        1951.

5. McCalla, T. R., "Reference Manual for FXAOSPM Vector Fix
        Program," Naval Security Group Activity, Skaggs
        Island, Sonoma, California, September 1970.

6. Pope, J. W. R., "A Vector Fix Procedure for High Fre-
        quency Direction Finding," Naval Security Group
        Activity, Skaggs Island, Sonoma, California,
        February 1971.

INITIAL DISTRIBUTION LIST

No. Copies

1. Chief of Naval Personnel   1
    Pers 11b
    Department of the Navy
    Washington, D.C.   20370

2. Commander, Naval Security Group Command   2
    (G53,G54)
    3801 Nebraska Ave., NW
    Washington, D.C.   20390

3. Commander, Oceans Systems Command Atlantic   1
    Box 100   (Attn: Captain C. E. Woods, USN)
    U.S. Naval Station Norfolk
    Norfolk, Va.   23511

4. Commanding Officer, Naval Security Group Activity   1
    Skaggs Island
    Sonoma, California   95476

5. Defense Documentation Center   2
    Cameron Station
    Alexandria, Virginia   22314

6. Director, Naval Research Laboratory   1
    PM-16 SPO
    Washington, D.C.   20390

7. Library, Code 0212   2
    Naval Postgraduate School
    Monterey, California   93940

8. Naval Postgraduate School   1
    Department of Operations Research and
      Administrative Sciences
    Monterey, California   93940

9. Professor Robert R. Read   1
    Department of Operations Research and
      Administrative Sciences
    Naval Postgraduate School
    Monterey, California   93940

10. Associate Professor Robert N. Forrest   1
    Department of Operations Research and
      Administrative Sciences
    Naval Postgraduate School
    Monterey, California   93940

11.   LT Ronald L. Potts, USN   1
      Box 1935
      Naval Postgraduate School
      Monterey, California 93940

DOCUMENT CONTROL DATA - R & D		
(Security classification of title, body of abstract and indexing annotation must be entered when the overall report is classified)		
1 ORIGINATING ACTIVITY *(Corporate author)*	2a. REPORT SECURITY CLASSIFICATION	
Naval Postgraduate School Monterey, California 93940	Unclassified	
	2b. GROUP	

3 REPORT TITLE

RADIO DIRECTION FINDING FIX SOLUTION IN SPHERICAL TRIGONOMETRY
WITH CONFIDENCE REGION AND LOCATION ERROR ANALYSIS

4 DESCRIPTIVE NOTES *(Type of report and inclusive dates)*

Master's Thesis; March 1973

5. AUTHOR(S) *(First name, middle initial, last name)*

Ronald L. Potts; Lieutenant, United States Navy

6. REPORT DATE	7a. TOTAL NO. OF PAGES	7b. NO. OF REFS
March 1973	112	6
8a. CONTRACT OR GRANT NO.	9a. ORIGINATOR'S REPORT NUMBER(S)	
b. PROJECT NO.		
c.	9b. OTHER REPORT NO(S) *(Any other numbers that may be assigned this report)*	
d.		

10. DISTRIBUTION STATEMENT

Approved for public release; distribution unlimited.

11. SUPPLEMENTARY NOTES	12. SPONSORING MILITARY ACTIVITY
	Naval Postgraduate School Monterey, California 93940

13. ABSTRACT

Although parts of this paper may be applicable to various
other location finding systems, radio direction finding was
selected for development because of the extensive literature
available on the subject. Using a modification of the navi-
gation coordinate system, equations in spherical trigonometry
are developed by analogy with graphical solution procedures.
Ellipticity of the earth is corrected for by use of geocentric
latitude in all calculations. The least squares solution is
found by a combination of second-order gradient searches and
Golden Section Searches on the corrected sphere. A Chi-Square
contour confidence region is presented with defense against
the empty region arguments and with verification of its
reliability of target containment. Sensitivity of location
error to network layout, number of measurements available
and intercept geometry factors is examined by computer
simulation, demonstrating the predictive value of these
statistics. It is shown that the correlation between
location error and the size of a reliable confidence
region is too minimal to have predictive value.

DD FORM 1473 (PAGE 1)
1 NOV 65
S/N 0101-807-6811
111
UNCLASSIFIED
Security Classification
A-31408

KEY WORDS	LINK A		LINK B		LINK C	
	ROLE	WT	ROLE	WT	ROLE	WT
CHI-SQUARE CONTOUR CONFIDENCE REGION						
CONFIDENCE REGION						
DIRECTION FINDING NETWORKS						
GEOCENTRIC LATITUDE						
GOLDEN SECTION SEARCH						
HIGH FREQUENCY DIPECTION FINDING						
INTERCEPT GEOMETRY						
LEAST SQUARES FIX SOLUTION						
LOCATION ACCURACY PREDICTION						
LOCATION ERROR ANALYSIS						
LINES OF POSITION						
POSITION LOCATING						
RADIO DIRECTION FINDING						
SEARCH REGION						
SECOND-ORDER GRADIENT SEARCH						
SIMULATION						

DD FORM 1473 (BACK)
1 NOV 65

:N 0101-807-6821

112

UNCLASSIFIED

Security Classification

A-31409